Published in final edited form as:
Biochim Biophys Acta. 2011 July ; 1807(7): 788–802. doi:10.1016/j.bbabio.2011.02.006.

The Q Cycle of Cytochrome *bc* Complexes: a Structure Perspective*

William A. Cramer[1,‡], **S. Saif Hasan**[1], and **Eiki Yamashita**[2]

[1] Hockmeyer Hall of Structural Biology, Department of Biological Sciences, Purdue University, West Lafayette, IN 47907, USA

[2] Institute for Protein Research, Osaka University, Suita, Osaka 565-0871, Japan

Summary

Aspects of the crystal structures of the hetero-oligomeric cytochrome bc_1 and b_6f ("bc") complexes relevant to their electron/proton transfer function and the associated redox reactions of the lipophilic quinones are discussed. Differences between the b_6f *and* bc_1 complexes are emphasized.

The cytochrome bc_1 and b_6f dimeric complexes diverge in structure from a core of subunits that coordinate redox groups consisting of two bis-histidine coordinated hemes, a heme b_n and b_p on the electrochemically negative (n) and positive (p) sides of the complex, the high potential [2Fe-2S] cluster and c-type heme at the p-side aqueous interface and aqueous phase, respectively, and quinone/quinol binding sites on the n- and p-sides of the complex. The bc_1 and b_6f complexes diverge in subunit composition and structure away from this core. b_6f also contains additional prosthetic groups including a *c*-type heme c_n on the n-side, and a chlorophyll *a* and β-carotene. *Common structure aspects; functions of the symmetric dimer*. (**I**) *Quinone exchange with the bilayer*. An inter-monomer protein-free cavity of approximately 30 Å along the membrane normal × 25 Å (central inter-monomer distance) × 15 Å (depth in the center), is common to both bc_1 and b_6f complexes, providing a niche in which the lipophilic quinone/quinol (Q/QH_2) can be exchanged with the membrane bilayer. (**II**) *Electron transfer*. The dimeric structure and the proximity of the two hemes b_p on the electrochemically positive side of the complex in the two monomer units allow the possibility of two alternate routes of electron transfer across the complex from heme b_p to b_n,: intra-monomer, and inter-monomer involving electron cross-over between the two hemes b_p. A structure-based summary of inter-heme distances in seven *bc* complexes, representing mitochondrial, chromatophore, cyanobacterial, and algal sources, indicates that, based on the distance parameter, the intra-monomer pathway would be favored kinetically. **(III)** *Separation of quinone binding sites.* A consequence of the dimer structure and the position of the Q/QH_2binding sites is that the p-side QH_2 oxidation and n-side Q reduction sites are each well separated. Therefore, In the event of an overlap in residence time by QH_2 or Q molecules at the two oxidation or reduction sites, their spatial separation would result in minimal steric interference between extended Q or QH_2 isoprenoid chains. **(IV)** *Trans-membrane QH_2/Q transfer*. (**i**) n/p side

*The theme of this manuscript was originally presented in a keynote lecture, November, 2009, for the Symposium commemorating the 50th anniversary of the Institute for Protein Research, Osaka University.

‡corresponding author: William A. Cramer, Hockmeyer Hall of Structural Biology, Department of Biological Sciences, Purdue University, West Lafayette, IN 47907, USA; Tel. 1-765-494-4956; Fax: 1-765-496-1189, waclab@purdue.edu.

QH_2/Q transfer may be hindered by lipid acyl chains; **(ii)** the shorter less hindered inter-monomer pathway across the complex would not pass through the center of the cavity, as inferred from the n-side antimycin site on one monomer and the p-side stigmatellin site on the other residing on the same surface of the complex. **(V)** *Narrow p-Side portal for QH_2/Q passage*. The [2Fe-2S] cluster that serves as oxidant, and whose hisitidine ligand serves as a H^+ acceptor in the oxidation of QH_2, is connected to the inter-monomer cavity by a narrow extended portal, which is also occupied in the b_6f complex by the 20 carbon phytyl chain of the bound chlorophyll.

Keywords

cytochrome bc_1; b_6f complex; electron transfer; energy transduction; membrane protein complex; plastoquinone; electrochemical potential; ubiquinone

I. Introduction

With the availability of crystal structures of the hetero-oligomeric cytochrome bc_1 (1–15) and b_6f (16–20) complexes, and of the extrinsic soluble domain of the Rieske iron-sulfur protein (21–25) from both complexes and of cytochrome *f* from the higher plant b_6f complex (26–30), pathways of electron and proton transfer and of quinone/ol entry and binding can be considered in the context of atomic structures. Properties that are common to both sets of complexes, or unique to either the bc_1 or b_6f set, can be defined. These comparisons can be used to describe the evolution of these complexes (31–37). Recent reviews and discussions have mostly focused either on the bc_1 (38–64) or the b_6f complex (65–76, 37, 77), with some on both complexes (78–80). It has often been assumed in discussions of the bc_1 complex that the differences in the structure and prosthetic groups of the two classes of complexes are inconsequential, and that the complexes do not differ significantly in pathways of electron and proton transfer. It will be emphasized in the present discussion that, although the bc_1 and b_6f complexes share a common evolutionary origin and many common functions, significant differences exist between the two sets of complexes with respect to details of structure, alternate electron transport pathways, and quinone-mediated redox function.

Structure-function problems discussed recently for the bc_1 complex include the role of the monomer and dimer in the electron transport pathway associated with oxidation of ubiquinol (56–58, 81) the redox state of the quinone species bound to the n-side of the complex (35, 53, 80), inter-monomer interactions that may affect the pathway of electron transfer (45, 82, 57), and consideration of a stochastic approach to a description of the electron transfer reactions in the Q cycle (61).

Recent review topics on the b_6f complex have included unique aspects of structure-function: (**i**) The photosystem I-linked cyclic electron transport pathway (83–99), absent in mitochondria and purple photosynthetic bacteria that house the bc_1 complex. An uncertainty over the participation of the b_6f complex in the cyclic pathway of oxygenic photosynthesis is based on disagreement over whether the quinone-analog inhibitor, antimycin A, which is a classical inhibitor of the oxidation of mitochondrial cytochrome *b* (100), and which inhibits cyclic phosphorylation (101, 102), does (103) or does not (102) inhibit turnover of the chloroplast heme b_n; (**ii**) the additional heme c_n in the b_6f complex, which was first described by sensitive spectrophotometry (104, 105), and subsequently in crystal structures (16, 17); (**iii**) FNR bound peripherally to the plant b_6f complex may participate along with heme b_n, in the cyclic electron transport pathway (106, 88).

An understanding of intra-membrane translocation of the large lipophilic Q/QH_2 (quinone/quinol) molecules, which is coupled to electron and proton transfer, involves consideration of formidable structure problems. Charge transfer, steric, and kinetic problems associated with quinone translocation across the membrane and the *bc* complex were recognized (107–111) in the literature that preceded the emergence of crystal structures of the *bc* complexes.

II. Cytochrome bc_1 and b_6f complexes; common and unique properties

Crystal structures of the hetero-oligomeric cytochrome *bc* complexes, which have a similar energy transducing function in respiration and photosynthesis, are summarized in Figs. 1A–C, the bc_1 complex from (**A**) yeast mitochondria (15) and (**B**) the purple photosynthetic bacterium, *Rb. sphaeroides*, and (**C**) the b_6f complex from the cyanobacterium, *M. laminosus* (19). These membrane protein complexes provide the electronic connection between the reducing (dehydrogenase, bacterial photosynthetic reaction center, or photosystem II reaction center) and oxidizing (cytochrome oxidase or photosystem I) electron transport complexes in the respective electron transport chains, while coupling electron transfer within the complex to proton translocation across the membrane. Genomic and hydrophobicity (112) analysis of the cytochrome *b* subunit allowed prediction of *bis*-histidine ligation of the two trans-membrane hemes in the N-terminal heme binding domain of the cytochrome *b* polypeptide in the hydrophobic core of the complex (113, 31, 114, 115), which was inferred to be identical in the b_6f and bc_1 complexes (31), and subsequently corroborated by crystal structures. The Rieske (116) iron-sulfur protein (ISP) subunit of the complex can also be considered part of its basic assembly (33, 117), as it is found in cytochrome *bc* complexes in a wide range of phylla (118), and phylogenetic reconstruction has shown significant congruence of ISP and cytochrome *b* (119) although the ISP amino acid sequences are less conserved than those of cyt *b* (23).

Structures, prosthetic groups

Cytochrome *bc* complexes contain four common redox prosthetic groups (Table I) in their redox core: (**i**) two *bis*-histidine coordinated *b* hemes, b_p and b_n (113, 31) whose His ligands bridge two trans-membrane alpha-helices, the 2^{nd} and 4^{th} of the cytochrome *b* polypeptide on the p- and n-sides of the complex (113, 31, 114). The pattern of heme bridging two trans-membrane helices via two His residues is a frequent structure motif, as subsequently found in the crystal structures of intra-membrane electron transport proteins, such as heme *b* in fumarate reductase (120) or formate dehydrogenase-N (121) and heme *a* in cytochrome oxidase (122–125); (**ii**) a high potential ($E_m \approx +0.25$- 0.35 V) *c*-type heme that is covalently bound in the p-side aqueous phase domain to the cytochrome *f* and c_1 polypeptides, where it serves as the electron acceptor of the [2Fe-2S] cluster. The iron-sulfur protein, through this cluster, is the electron acceptor and, through a histidine ligand, a proton acceptor of ubi- or plastoquinol at the p-side membrane interface. A newly discovered feature of *b*-heme orientation in b_6f complexes (20) is that heme b_p in *M. laminosus* (PDB: 2E74) is rotated 180° about the normal to the membrane plane relative to the heme orientation in *Nostoc* (PDB, 2ZT9) and *C. reinhardtii* (PDB,1Q90). This heme rotation phenomenon has been noted previously and discussed in the context of *bis*-histidine coordination geometry in trans-membrane 4-helix bundles (126).

Although cytochrome bc_1 *and* b_6f complexes possess a common core of four redox groups consisting of the high potential [2Fe-2S] cluster, 2 trans-membrane *b* hemes, and a heme-binding protein core with a common evolutionary origin, the similarity in the structure decreases away from this core. In addition, bc_1 and b_6f complexes both contain a high potential *c*-type heme whose presence in both complexes is a result of convergent evolution (27). there are four additional tightly bound prosthetic groups found in b_6f complexes that are not present in bc_1: (**i**) a 4^{th} heme and 5^{th} redox group, the heme c_n, also called c_i in the

literature (e. g., (17)), originally described by sensitive spectrophotometric analysis of electron transport reactions of the b_6f complex *in situ* and *in vivo* (104, 105). Heme c_n was defined in the crystal structures that showed it covalently bound to the n-side of helix A of the cytochrome *b* subunit, with its heme Fe within 4 Å of a propionate oxygen of the adjacent heme b_n (16, 17). This proximity predicts electronic coupling between hemes b_n and c_n, which is verified by a unique EPR spectrum containing a g ~ 12 signal (127–129). Given this degree of electronic coupling, it is surprising that hemes b_n and c_n have been found to possess distinct redox potentials (130). However, because heme c_n has a midpoint redox potential similar to that of heme b_n in the bc_1 complex (130), $b_n - c_n$ could function in the Q cycle on the n-side of the b_6f complex as a two electron donor to the n-side bound quinone, Q_n (see below, Figs. 3A, B). In addition, from crystal structures (19) and redox titrations in the presence of NQNO (130), heme c_n is inferred to function as the n-side quinone binding site (19), and as a possible binding site for O_2 (129). A mutation of interest in the heme maturation pathway of heme c_n resulted in low levels of b_6f complex (131, 132), which could be overcome by a spontaneous revertant missing a protease. A double mutant made in a background of the protease-less mutant was constructed that functions at a low rate in the absence of heme c_n (133). Three additional prosthetic groups unique to the b_6f complex are: (**ii**) chlorophyll *a* (134–136) (**iii**) β-carotene (136), and (**iv**) a flavin in the FNR subunit of the plant (spinach) complex (137, 138, 106, 96).

Other unique structure features of the b_6f compared to the bc_1 complex include: (**v**) completely different structures of the extrinsic domain of cytochromes c_1 and *f* (26–28), except for the Cys-X-Y-Cys-His covalent heme binding sequence, and (**vi**) four small single trans-membrane helical subunits in a “picket-fence” arrangement at the periphery of each monomer of the b_6f complex (16–20).

Polypeptides

Of the 8 and 11 polypeptide subunits that have been defined in the crystal structures of b_6f and respiratory bc_1 complexes, respectively, 3–4 that contain the functionally essential redox groups can be considered “core” polypeptides. They contain binding sites for the redox prosthetic groups, the 2 b hemes, the {2Fe-2S] cluster, the high potential c-type heme, the n- and p-side quinone binding sites. These subunits define the hydrophobic core that corresponds to the 3–4 subunit structure of the bc_1 complex of the purple photosynthetic bacterium, *Rb. sphaeroides* (14). *Additional interacting and/or bound polypeptides*. a complete perspective on the atomic structure of the *bc* complexes should include the less strongly or transiently bound subunits that may be dissociated and lost from the complex during its isolation, purification, or crystallization. For the b_6f complex, these include: (i) the FNR that is found in the plant, but not the cyanobacterial or algal b_6f complex (137, 138, 106); (ii) the petP polypeptide seen in cyanobacteria (139); and (iii) the light-harvesting LHCII chlorophyll protein kinase Stt7-STN7 (140), whose presence on the n-side or stromal side of the complex may respond to quinol oxidation on the p-side (141, 142), the correlated (iv) phosphatase (143); and (v) the petO nuclear-encoded phosphorylatable subunit (144).

The inter-monomer cavity

A prominent common feature in the structure of bc_1 and b_6f complexes is the large (30 Å × 25 Å × 15 Å) central cavity which, because of its presumed role in sequestering quinone from the membrane bilayer, has been termed the “quinone exchange cavity”(16). As discussed below, the term “cavity” may be a misnomer because it is likely that it is mostly filled with lipid acyl chains. Central cavities in dimeric or pseudo-dimeric membrane proteins that sequester substrates and water are found in the structures of transport proteins such as the lac permease (145) and the glycerol-3-phosphate transporter (146).

Lipids

At least eleven lipid molecules have been defined in the 1.9 Å structure of the yeast bc_1 complex (147, 148, 50, 59, 15, 62), i.e., 5 1/2 lipids per monomer. Each monomer also contains one peripheral CL, two phosphatidyl-ethanolamines, and two phosphatidic acids (Figs. 2A, B). An additional potential lipid site in each bc_1 monomer is suggested by the presence of one bound undecyl-maltoside detergent molecule. One n-side cardiolipin (CL) is shared between the N-terminal segment of the cytochrome *b* subunit in each monomer, with a proposed function of a proton antenna for H^+ - coupled reduction of the n-side quinone, Q_n (59, 149, 62). Considering this putative function, the distance between the quinone keto group (seen in the 1NTZ structure) and the nearest CL phosphate oxygen is 10.5 Å, a very large distance for proton transfer (150). The distance for proton hopping is reduced by the presence of His202 (cyt *b*) between the CL phosphate O and the protonatable nitrogen of the cyt *b* His202.

A similar number, 7–8 lipid binding sites per monomer, is seen in b_6f complexes from the cyanobacteria, *M. laminosus* (19) *and Nostoc* sp. PCC 7120 (20). One of these sites in the b_6f complex is occupied by a natural sulfo-lipid, first seen in the structure of the *C. reinhardtii* complex (17), whose interaction with n-side segments of the ISP and cytochrome *f* has been described (151). The other six lipid binding sites in the monomer of the *M. laminosus* structure are occupied by four molecules of the detergent UDM and two of the lipid DOPC, whose presence greatly increased the rate of crystal formation of delipidated b_6f complex (152). Two additional "natural" lipids, MGDG, for a total of three lipids/ monomer, have been assigned in the *C. reinhardtii* b_6f complex (17). Regarding application of the "H^+ antenna hypothesis" (59, 149, 62) to the b_6f complex, there are 2 UDM molecules per dimer near the position of the inter-monomer cardiolipin, CL, in the b_6f complex. These UDM detergent molecules may replace the natural lipid molecules, e. g., anionic PG, in the detergent-extracted protein complex. Of the four UDM molecules in each monomer, the head groups of three are pointing to, or are in contact with, the n-side aqueous phase. Arg207 and Lys208 intervene as possible H^+ carriers in the path between the O (OAC) of the quinone analogue, decyl-stigmatellin, which can bind to the Q_n site in b_6f (19), and UDM as a putative substitute for CL.

Inter-monomer interactions; conformational changes

The ability of one equivalent added per dimer of the p-side quinone analogue inhibitor, stigmatellin, to completely inhibit electron transfer of the dimeric yeast bc_1 complex, led to the inference of inter-monomer interactions relevant to the electron transfer mechanism of the dimer (45). A similar "half-sites" inhibition effect in the b_6f complex has been observed in photosynthetic electron transport, using the p-side inhibitor, DBMIB (153), whose structural basis could be similarly interpreted. The structural basis for inter-monomer interactions and resulting conformational changes, which could be at the root of these "half-site" effects and those observed for the bc_1 complex from yeast (45, 154, 57) and *P. denitrificans* (63), may be contained in the number and nature of the residues involved in close contacts between monomers in bc_1 and b_6f complexes (Table 2). The number of residues contributed to such interactions by core subunits, (**i**) cytochrome *b* (8 trans-membrane helices) and the ISP of the bc_1 complex, and (**ii**) cytochrome *b (*4 TMH*)*, subunit IV (3 TMH), and the ISP of the b_6f complex, are similar in the two complexes. The larger number of interacting residues in the yeast (3CX5) and bovine (1NTZ) bc_1 complexes, compared to the two cyanobacterial b_6f complexes, is a consequence of a larger number of bc1 TMH making inter-monomer contacts: (**a**) the TMH of cytochrome c_1 makes inter-monomer contact, but that of cytochrome *f* doesn't; (**b**) the small subunits in bc_1 make contacts, but the four small subunits in b_6f, the petG, L, M, N subunits, which are at the outside periphery of each b_6f monomer, with one TMH each, do not. One TMH in each

monomer with unusual properties is that of the Rieske ISP, whose active p-side [2Fe-2S] cluster in one monomer is connected to its TMH by a long glycine-rich disordered flexible loop that spans the trans-membrane domain of the other at a pronounced oblique angle (Figs. 1A–C; described in yellow).

Extensive conformational changes of the [2Fe-2S]-containing sub-domain of the Rieske ISP are necessary to accomplish kinetically competent electron transfer from the [2Fe-2S] cluster to the heme of cytochrome c_1 or *f* (3). For both complexes, the [2Fe-2S] donor – heme c acceptor distance, derived from structures described in PDB 3CX5 and 2E74, 22.5 Å and 26.1 Å (seen "edge-edge" in Figs. 5A, B) is too large for competent electron transfer. These distances would result in electron transfer times that are at least1000 times larger than the ~ msec rate-limiting step of the system (155). Different crystal forms of bc_1 complex show conformations with shorter [2Fe-2S] - heme c_1 distances (12.8 Å, 3H1H, (5) and 15.5 Å, 1BE3, (4, 156)) that would allow kinetically competent electron transfer (5). The 15.5 Å distance described in PDB 1BE3, the cyt c_1-proximal conformation, is one of three crystallographically determined [2Fe-2S] - heme c_1 distances between the [2Fe-2S] cluster and the cyt c_1 heme that have been defined in the bovine complex. The others are 31.6 Å in the heme b_p-proximal conformation (PDB, 3BCC) and 27.5 Å in an "intermediate" conformational state (PDB, 1BGY (4)). These structure data imply protein conformational changes ISP that cause the [2Fe-2S] cluster to alternate between positions that are distal and proximal to the heme of cyt c1, the latter allowing competent electron transfer.

The rotation-translation of the cluster-containing peripheral sub-domain of the Rieske protein in the bc_1 complex is enabled by rotation-translation about the flexible linker region that connects the peripheral domain in one monomer with the trans-membrane α-helix in the other. The necessity of flexibility in this loop was demonstrated through site-directed mutations that are predicted to result in structure changes that decrease the mobility of this linker region (157–159, 43). Substitutions of multiple proline or glycine residues in the loop region of the b_6f complex, or insertions that caused loop elongation had no effect on activity (160), although these mutations are similar to those cited above that markedly decreased activity of the bc_1 complex. A crystal structure to demonstrate the cyt *f* heme-proximal state of the {2Fe-2S] cluster in the b_6f complex, which would be necessary for kinetically competent activity, has not yet been determined.

Inhibitor-induced conformational changes

(**a**) *p-side quinone analogue inhibitors*. For the bc_1 *complex*, the inhibitor stigmatellin, which binds in the p-side entry portal close to an imidazole ligand of the ISP [2Fe-2S] cluster, is present in almost all crystal structures because its presence results in decreased mobility {Kim, 1998 #257} and increased order of the ISP soluble domain, although it does not change the orientation of the cluster itself (161). For cyt b_6f, a structure of the native complex without any bound inhibitor has been obtained (20). Large conformational changes of the b_6f complex induced by stigmatellin have been reported in a study with 2D crystals (162), although such changes were not seen in a comparison of 3D crystals, native vs b_6f with stigmatellin (19), for which the RMSD for the 2E74 vs. 2E76 (+ tridecyl-stigmatellin) structures from *Nostoc* is 1.18 Å. (**b**) *n-side inhibitors*. RMSD changes of significant amplitude associated with the binding of the known specific inhibitors have not been detected: **(i)** the RMSD of the native (1NTM) vs. antimycin A-inhibited (1NTK) bovine bc_1 complex is 0.47 Å; (**ii**) for *Nostoc* b_6f structures, the RMSD of 2E74 vs. 2E75 (+ NQNO) is 0.43 Å (19). **(iii)** the RMSD for the avian bc_1 complex, stigmatellin vs. stigmatellin and antimycin is 0.36 Å (PDB, 3H1J vs 3H1I). However, antimycin causes a 100 -150 mV change in the E_{m7} of a mitochondrial *b* heme (163), presumably heme b_n, and a perturbation of the p-side EPR signal associated with the [2Fe-2S] cluster in the bc_1 complex of the photosynthetic bacterium, *Rb. capsulatus* (164, 165, 64).

III. The Q cycle

The coupling of the oxidation-reduction and deprotonation-protonation of lipophilic quinone/ol (Q/QH_2) within the cytochrome *bc* complex is central to the mechanism of proton translocation in the complex. The proton/electron carriers, ubiquinone (UQ-10; (166, 167)) in the respiratory bc_1 complex, and plastoquinone (PQ-9) in the b_6f complex contain 10 and 9 isoprenoid groups, respectively. In the extended state, steric problems are anticipated in translocation of these quinones in a rigid extended state across the cytochrome *bc* complex, or their reversible insertion into oxidative or reductive niches within the complex. Possible conformational transitions to folded states have been described (168–170). Based on the observation of oxidant-induced reduction of *b*-type heme in the respiratory bc_1 complex (171), it was proposed that these quinones can cross the cytochrome *bc* complex and the membrane, as described in the "Q cycle" models proposed by Mitchell (172–174), and in subsequent discussions of this model (175, 109, 111, 176, 46, 80). Descriptions of the Q-cycle that illustrate differences between bc_1 and b_6f complexes are shown (Figs. 3A, B). Other formulations of the Q cycle are found in (177, 51, 53, 80).

Experimental data that were fundamental to the formulation of the Q cycle models are: (**a**) oxidant-induced reduction of cytochrome *b* of the mitochondrial respiratory complex(171, 178, 179); (**b**) a proton:electron ratio, $H^+/e = 2$, for uncoupler-sensitive electrogenic proton translocation to the p-side aqueous phase by the bc_1 (180, 181) and b_6f (182) complexes in the presence of a relatively small $\Delta\mu_{H^+}$ (183, 184) (for the b_6f complex, there has been debate as to whether the extra H^+ translocation, which is electrogenic, is inhibited in the presence of a large $\Delta\tilde{\mu}H^+$ (185), and whether it is (105, 186) or isn't (187–189) specifically associated with the reduction of the hemes *b*). (**c**) The model is also strongly supported by the presence of specific Q binding sites of potent quinone analogue inhibitors, e. g., antimycin A and stigmatellin, on both n and p sides of the complexes, whose precise locations have been confirmed by: (**i**) crystal structures; ubiquinone (PDB, **3H1H**) or antimycin (PDB, **3H1I**) binding sites have been determined on the *n*-side of the complex adjacent to heme b_n, and stigmatellin binding site on the *p*-side (PDB: **3H1J**) within H-bond distance of the histidine ligand (His181 in yeast) to one of the Fe atoms in the [2Fe-2S] cluster. In the b6f complex, analogous n- and p-side binding sites of NQNO and tridecyl-stigmatellin have been identified (19). (**ii**) EPR detection of a ubisemiquinone free radical intermediate, in the absence, but not in the presence of antimycin (190), and an analogous oxygen-sensitive p-side signal (191).

Independent data supporting the Q cycle model for redox and H^+ transfer reactions in the b_6f complex are less complete because: (**i**) there is no high affinity n-side inhibitor comparable to antimycin A for the bc_1 complex, which is partly a consequence of partial occupancy in the b_6f complex of the bc_1-like Q_n site by heme c_n (19); (**ii**) in contrast to the bc_1 complex, the alpha-band absorbance spectra of the two trans-membrane hemes, b_p and b_n, cannot readily be distinguished (e. g., (105); although see (192)). Together with the fact that any ΔE_m between the two hemes is much smaller in the b_6f complex compared to bc_1, and not resolved in most in situ titrations, a determination of the sequence of reduction of the two hemes in b_6f, as accomplished for bc_1 in chromatophores of the photosynthetic bacteria (193, 194), is precluded.

(iii). *The rate-limiting step:* From studies on the bc_1 complex in *Rb. sphaeroides*, it was inferred that transfer of the first electron in the two electron quinol oxidation to the ISP, in a proton-coupled electron transfer (195), is the rate-limiting step of the overall Q cycle (48, 196) (Figs. 3A, B).

Electron and proton reactions of the bc_1 and b_6f complexes in the context of a Q cycle are summarized (Table 3A1, 2). The presence of the unique heme c_n, whose covalent attachment to the cytochrome *b* polypeptide can be detected in SDS-PAGE analysis of the b_6f complex (197), and which is electronically coupled to heme b_n (127, 128), makes the detailed nature of a "Q cycle" different in the b_6f complex compared to bc_1: (i) Crystal structures and spectrophotometric analysis showing quinone analogue inhibitors NQNO (130, 128, 19) and tridecyl-stigmatellin (19) as ligands to heme c_n imply that heme c_n is the n-side PQ binding site. The electronically coupled hemes b_n/c_n could provide a 2 electron pathway for reduction of PQ_n. The presence of NQNO and stigmatellin as ligands to heme c_n, as defined in crystal structures (2E75, 2E76; (19)) implies a role in the n-side electron transfer reactions (Table 3B, n-side reactions, **ii**–**iv**). The isolation of a plant (spinach) b_6f complex from the green alga *C. reinhardtii,* containing bound ferredoxin-$NADP^+$ reductase (FNR) (106), and of a supercomplex containing the PSI reaction center and b_6f complexes together with FNR (96), implies the possibility that PSI-linked cyclic electron transport provides an alternative source of electrons into the b_6f complex. An FNR-dependent reductive pathway to PQ_n resembles an original formulation of the Q cycle for the bc_1 complex, in which the one of the two electrons needed for reduction of UQ_n was suppled by an n-side dehydrogenase (173).

The cyclic pathway may be augmented by an NADH dehydrogenase, implied by studies on chloroplast mutants in *Arapidopsis thaliana* (97). Regardless of the source of electrons from the cyclic pathway, it is proposed that the Q cycle in the b_6f complex could be completed on the n-side by one electron supplied by the cyclic pathway (Table 3, B3, v), which would complement the electron derived from the p-side oxidation of plastoquinol. The possibility can also be considered that two electrons stored on hemes b_n-c_n cooperatively reduce PQ (PQ_n) bound at the site proximal to heme c_n (Table 3, B3, vi) to PQH_2. A consequence of the input of one electron from cyclic electron transport to reduce Q_n is that only one p-side oxidative turnover of PQH_2 would be required to from Q_nH_2.

Another ("activated") Q cycle model (53) (Table 3, B4) proposes that the quinone species bound at the Q_n site is a semiquinone, which can form a complex and transfer an electron to the higher potential heme b_n (*b*-150; (198, 199)) on the other monomer. This most recent and interesting formulation of a modified Q cycle results from consideration of a substantial number of experiments, mainly concerning the flash-induced amplitude and kinetics of the trans-complex electric field and heme *b* reduction that do not fit the models described in Table 3A1-3, 3B1, 2. The "activated" mechanism employs the dimeric *bc* complex, in which prompt oxidation of the quinol on the n-side of one monomer reduces heme b_n on the other. The mechanism then requires only one oxidation (turnover) of Q_pH_2 to provide the single electron needed to form the quinol Q_nH_2 and once primed, minimizes exchange of QH_2/Q with the membrane QH_2/Q pool. This mechanism was originally proposed for the bc_1 complex (53), and subsequently for the b_6f complex (80). Two problems with application to the b_6f complex are: (**i**) the E_m of heme b_n in b_6f (Table 1) is approximately 100 mV more negative than that in bc_1 (Table 1), implying a less favorable equilibration between bound Q_n semiquinone and heme b_n than would occur in the bc_1 complex, assuming that the Q_n semiquinone has the same E_m in both systems; (**ii**) the large distance (pdb: 1NTZ) (10)), 28 Å in bovine bc_1, between the ring of the quinone at the Q_n site in one monomer and heme b_n in the other would result in a very slow (time scale of seconds) electron transfer step in the cycle, suggesting a kinetic difficulty.

IV. Pathways for quinone transfer; consequences of dimer symmetry

Given the above data and logic that are consistent with, and support, the Q cycle models shown in Figs. 3A, B with the electron and proton transfer reactions described in Table 3, it

is noted that there are no data available on the pathway or trajectories of the lipophilic quinone/ol (Q/QH2) within the *bc* complex connecting its n and p sides. Then, it is important to consider in the context of the atomic structures of the *bc* complexes (Figs. 1A–C), the possible trans-membrane pathways used by the long chain lipophilic quinones/ quinols to transfer electrons and protons within the *bc* complexes.

Quinone binding in the dimer; consequences of symmetry

Although intra-complex transfer of Q, QH_2, and semiquinone has been proposed, and is implied in many models of the Q cycle (175, 109, 111, 176, 46, 80), the presence of lipid acyl chains within the inter-monomer cavity is indicated by at least 11 bound lipids resolved in the yeast complex (3CX5), and an Fo – Fc map of the inter-monomer cavity indicating additional lipid acyl chains (Fig. 4A). It is likely that the cavity is occupied by an even higher density of lipid chains than shown, but that most of this lipid is weakly bound and lost during purification and crystallization. The presence of this lipid implies that intra-complex transfer of Q/QH_2 through the inter-monomer cavity might be impeded by the lipid chains, although such obstruction would be lessened by the disorder and probable mobility of these chains. Furthermore,_a consequence of the C2 symmetry is that the two monomers are arranged so that: (**i**) the [2Fe-2S] quinol oxidation site and the quinone reduction site (b_n in the bc_1 complex and b_n-c_n in b_6f) in each monomers are on opposite faces of the complex (Fig. 4B); (**ii**) heme b_n in either monomer of the bc_1 complex, or hemes b_n-c_n in the b_6f complex, are on the same side of the complex as the 2Fe-2S cluster in the other monomer. Thus, the n-side binding site of antimycin on one monomer is on the same side of the dimeric complex as the p-side binding site of stigmatellin on the other (Fig. 4B), implying that if transfer of Q/QH_2 occurs across the *bc* complex, the transfer trajectory will be on one side of the complex (3, 41). (It is noted that the yeast 3XC5 structure does not have a true C2 symmetry because cytochrome c is bound to one monomer and the partly disordered cardiolipin shared on the n-side between the two monomers is asymmetrically located).

A side-view (Fig. 4C) of the yeast bc_1 complex (PDB 1KB9) shows an apparent cross-over of ubiquinone isoprenoid tail (UQ-6) bound at the Q_n site in one monomer across the inter-monomer cavity, to the Q_p site portal in the other monomer, which is located by stigmatellin (Stg; colored magenta). The cross-over is only apparent as the Stg and UQ-6 pair colored magenta is located on one face of the bc_1 dimer, while that colored green lies on the other.

Movement and transfer of the quinone(ol) through the complex will increase efficiency. However, there must be some exchange with the Q/QH_2 pool in the bilayer because 2 QH_2 are oxidized on the p-side for every Q that is reduced on the p-side. Therefore, two electrons (i. e., 2 equivalents of reductant) are lost from the complex, and one extra Q molecule is generated in every cycle. Therefore, even if one of the 2 Q generated from the oxidation of 2 Q_pH_2 is transferred across the cavity to the Qn site, the second Q_p must be released from the complex to the membrane bilayer, and a second Q_pH_2 supplied from the membrane bilayer to the oxidation site at the [2Fe-2S] cluster. Because the oxidation of the 2 QH_2 must occur in a few milliseconds, transfer of QH_2 from the photosystem II complex to b_6f must occur rapidly, suggesting the possibility of a supercomplex.

V. Role of the dimer in electron transfer

A dimeric or multimeric structure is a common structure motif in integral membrane proteins, prominent among which are the photosynthetic reaction centers (200–204). The electron and proton transfer reactions described in Table 3 do not describe any special function of the dimer. They do not distinguish whether electron transfer across the complex from heme b_p to b_n is (**a**) intra-monomer (58, 61) or (**b**) inter-monomer with cross-over between the two hemes b_p. The latter possibility was suggested after the appearance of the

crystal structures of the bc_1 complex that defined the inter-heme distances (78), and subsequently discussed extensively (154, 205–207, 82, 57, 56, 63). A "cross-over model" suggests that a function of the dimer could be to allow a "bypass valve" for a second pathway of trans-membrane electron transfer if the pathway for trans-membrane electron transfer in one monomer is impeded by reduction of the quinone in the Q_n binding site in that monomer, or by electron equilibration in that monomer. There are different quantitative descriptions of the electronic connection between the electron donor and acceptor, e. g., whether the distance separation between electron donor and acceptor should be measured "center to center" (208, 209) or "edge-edge" (210, 155, 211), the electron donor-acceptor distance, in addition to the free energy change, ΔG, and reorganization energy associated with the transfer (212–215) are major determinants of the branching ratio for intra-monomer vs. inter-monomer electron transfer (213). The crystal structures (Figs. 1A–C) provide donor-acceptor distances to an accuracy of ~ ± 0.3–0.5 Å (Table 4A, B) and the identity of the amino acids that bridge the potential electron transfer pathways (Figs. 5A–D). Heme edge-edge, ring-ring (bypassing side chains), and center-center (Fe:Fe) distances for seven bc_1 and b_6f structures are summarized in Table 4A, B. The seven structures include three bc_1 respiratory complexes: (**i**) yeast with bound stigmatellin and cytochrome c bound to one subunit [(15); 3CX5], (**ii**) bovine mitochondria with p-side bound stigmatellin and antimycin A (216); 2A06], (**iii**) bovine complex with n-side bound ubiquinone-2 (1NTZ); (**iv**) 3 subunit bc_1 complex from the photosynthetic bacterium, *Rb. sphaeroides*, with p-side bound stigmatellin (2QJP); (**v, vi**) native b_6f complex from the filamentous cyanobacteria, *M. laminosus* and *Nostoc* PCC 7120 (2E74, 2ZT9); (**vii**) b_6f complex from the green alga, *C. reinhardtii* with the p-side bound inhibitor stigmatellin (1Q90).

Split Soret band circular dichroism spectra of the mitochondrial bc_1 (217–219) and b_6f complex from *C. reinhardtii* b_6f (220), cyanobacteria and spinach chloroplasts (221), are diagnostic of heme-heme excitonic interactions that arise from the small inter-heme distances required for such interactions. For inter-monomer electron transfer, the only pathway considered is that between the two b_p hemes because of the large distance (~ 30 Å) in all cytochrome *bc* structures between the two hemes b_n and between heme b_n and b_p in different monomers. The pathway between the two b_p hemes, bridged by two Tyr residues and two Phe residues, respectively, in the bc_1 and b_6f complexes, approximately 10 Å in the yeast bc_1 complex and 13 Å in the *M. laminosus* b_6f complex is shown (Figs. 6C, D). For inter-monomer electron transfer, i. e., "cross-over," differences in edge-edge and ring-ring distances distance for closest contact between the two hemes b_p, relative to that between b_p and b_n, are (10.0–7.2) = 2.8 Å and (13.7 −12.2) = 1.5 Å, respectively, for the yeast respiratory bc_1 complex, which has the best resolution in the set (Figs. 1A, 6A (15); Table 4A, B). This comparison implies that the intra-monomer b_p-b_n pathway would be favored. The b_p- b_p edge-edge and ring-ring inter-monomer distances are also greater than the intra-monomer b_p - b_n distances for all six of the other representative bc_1 and b_6f complexes considered in Table 4A, B. The difference in the inter- vs. intra-monomer distances (determined edge-edge, ring-ring) are (2.7 Å, 1.5 Å) and (2.3 Å, 1.5 Å) for the bc_1 complexes described in 2QJP and 1NTZ, and (4.5, 3.1Å), (5.5 Å, 3.0 Å), and (3.8 Å. 2.9 Å) for the b_6f complexes described 2ZT9, 2E74, and 1Q90. Thus, for all seven cytochrome *bc* complexes, the intra-monomer distances, edge-edge and ring-ring, are clearly smaller than the inter-monomer distances. The differences for center-center distances show the same tendency, but are smaller and in some cases do not exceed experimental uncertainty. It is of interest that these inter-heme distances are the same for *bc* complexes from different sources and are not changed by the presence of n- or p-side quinol analogue inhibitors.

Considering only the distance dependence of the electron transfer rate, the difference in edge-edge and ring-distances would predict (210, 222, 208, 155, 223, 209, 224, 225, 211, 226, 227) a branching ratio for electron transfer from heme b_p that would significantly favor

the intra-monomer pathway. This logic is similar to that used previously to predict a branching ratio that favors the intra-monomer pathway by two orders of magnitude (215). The latter reference provides an extensive discussion of the intra/inter-monomer electron transfer problem, including the effect of the trans-membrane electric field generated by intra-monomer electron transfer that would inhibit the transfer. Recent studies using *b* heme knock-out mutants and splicing of the cytochrome b gene have demonstrated that the inter-monomer cross-over branching ratio is > 1 (81), and has been estimated to be 2–10 to 1 (228). Special functions associated with the inter-monomer cross-over pathway, discussed elsewhere for the bc_1 complex, have been mentioned above. For the b_6f complex, a selective pathway for electron transfer is implied from the observation that FNR in the presence of the "artificial" electron donor NADPH, reduces no more than half of the *b* heme in the b_6f complex (229, 19, 230). This half could be the heme b_n in the two monomers (229) or hemes b_n and b_p in one. Selection of the one monomer may result from interaction via n-side docking of an electron donating protein such as FNR (106) (Fig. 3B). In this case, because the chemical reduction is so slow (> seconds) and the half-reduction is an equilibrium level, an explanation solely in terms of differential kinetics of reduction based on differences in inter-heme distances is not adequate.

VI. The problem of the p-side portal

Passage of the lipophilic quinol to its oxidation and deprotonation site at the [2Fe-2S] cluster requires that after its entry into the inter-monomer cavity, or transfer from its n-side reduction site, it must pass through a narrow 15 Å long portal that is 10–12 Å and 13–14 Å wide at the cavity-side entrance in bc_1 and b_6f complexes. The nature of this portal for stigmatellin has been described for the yeast bc_1 complex (7). The portal is shown with an inserted p-side quinone analogue inhibitor, tri-decyl stigmatellin or stigmatellin (in green) in Figs. 6A, B for the cytochrome b_6f and bc_1 complexes, respectively. Such portals are also present in the Q_B quinone binding site of the bacterial (231, 232) and photosystem II photosynthetic reaction centers (204, 233). The overlap of tridecyl-stigmatellin and the phytyl chain of chlorophyll *a* also passing through the portal in the b_6f complex (*M. laminosus*; PDB, 2E76) is shown (Fig. 6C). An expanded view of the Q/QH_2 entry/exit portal showing residues within 4 Å of stigmatellin is shown in (Fig. 6D) for the yeast bc_1 complex. Stigmatellin, possessing a chromone ring that forms an H-bond with the His181 (bc_1; PDB, 3CX5) or His129 (b_6f; PDB, 2E76) ligand of the Rieske [2Fe-2S] cluster, and inhibits electron transfer from the cluster to the heme of cytochrome c_1 or *f*, was defined as a "class Ib" inhibitor (12). UHDBT is another inhibitor in this class. Myxothiazol and MOAS, which contain a β-methoxyacrylate ring, were classified as "1a" inhibitors (12); the binding of myxothiazol in the p-side portal is shown (Fig. 6E).

A better understanding of the insertion and passage of the lipophilic Q/QH2 through the portal could be gained through molecular dynamics analysis, as studied in the passage of ubiquinone through a defect in the ring of light-harvesting (LHI) bacteriochlorophyll molecules surrounding the photosynthetic reaction center (234), and the insertion of a drug molecule into a virus capsid protein (235), which has a formal resemblance to quinol insertion into the p-side entry portal to the [2Fe-2S] cluster. The combination of kinetic and steric constraints of portal entry-extrusion of quinol/quinone in the most frequent description of the Q cycle, described symbolically in Fig. 3A, creates a unique sequence of intra-membrane transfer events that occur twice in the msec turnover time of the bc_1 and b_6f complexes: **(i)** QH_2 with its isoprenoid chain of 45–50 carbons must find the narrow portal entry; **(ii)** traverse its narrow aperture, **(iii)** transfer 2 electrons and 2 protons; **(iv)** Q is extruded from the portal after oxidation and de-protonation, As the problem of entry into, and from, the portal is dynamic, different folded conformations (168, 169, 234) of the quinone may be relevant to the Q/QH_2 passage through the portal. As an indicator of the

conformational flexibility of the portal, the average B-factors (^{2}) of (**i**) portal residues and (**ii**) residues in neighboring trans-membrane helices are 27.2 and 25.8 for the 1. 9 Å yeast bc_1 complex with stigmatellin bound in the portal (3CX5), implying that the portal is relatively ordered in the presence of stigmatellin, an inference previously made for the yeast 2.3 Å structure (3EZV), with B factors (measures of disordered regions in the structure) of 37.0 and 35.2 Å^2, respectively, for the bound stigmatellin and neighboring portal residues (7). In contrast, for native b_6f complex solved in the absence of any quinone analogue inhibitor (2E74), the B factor (60.6 Å^2) for the residues lining the p-side portal is substantially larger than that, 44.7 Å^2, of residues in the neighboring trans-membrane helices, indicative of greater flexibility or disorder in the structure of the portal, which would facilitate passage of quinol/quinone or the analogue inhibitor. The greater order upon insertion of the quinone analogue inhibitor suggests that entry of the quinone or analogue requires interaction with the walls of the portal, which is reflected in the decreased B values.

In addition to the binding sites of stigmatellin (17, 19) and NQNO (19) defined in crystal structures of the b_6f complex, the high affinity binding site of the p-side quinone analogue inhibitor DBMIB (236) was found near the p-side aqueous interface, 19 Å from its site of inhibition at the [2Fe-2S] cluster (18). However, EPR analysis showed one high affinity site for DBMIB to be proximal to the [2Fe-2S] cluster (237, 238), and a second low affinity site further away from the cluster. DBMIB inhibition activated by light flashes implies that there is light-activated movement of DBMIB from the distal peripheral site to the inhibitory site proximal to the [2Fe-2S] cluster (239, 240). Thus, from its high affinity binding site determined in the crystal structure, DBMIB traverses a long and labyrinthine pathway to the [2Fe-2S] cluster where it exerts its inhibitory effect.

Acknowledgments

We thank H. Huang and C. B. Post for discussions on molecular dynamics of the quinone isoprenoid chain, and D. Baniulis, D. Beratan, F. Daldal, J. Hempel, F. Rappaport, S. Savikhin, S. D. Zakharov, and H. Zhang for helpful discussions. Studies of the authors related to this manuscript were supported by U. S. NIH GM-38323. Diffraction measurements associated with crystal structures of the b_6f complex were carried out with advice from S. Ginell, J. Lanarz, and F. Rotella at Beam-Line19-ID of the Structural Biology Center, Advanced Photon Source, Argonne National Laboratory, operated by the University of Chicago (contract DE-AC02-06CH11357, U.S. Department of Energy, Office of Biological and Environmental Research).

Abbreviations

b_n,Q_n and b_p, Q_p, hemes	quinone/ol bound on electrochemically negative or positive sides of membrane
n-	p-side (chloroplast stroma, lumen; mitochondrial matrix, inter-membrane space; bacterial cytoplasm ,periplasm)
CHARMM	*C*hemistry at *HAR*vard *M*acromolecular *M*echanics
CL	cardiolipin
cyt	cytochrome
DBMIB	2,5-dibromo-3-methyl-6-isopropylbenzoquinone
EPR	electron paramagnetic resonance
E_m,E_{m7}	mid-point oxidation-reduction potential, at pH 7
FAD	flavin adenine dinucleotide
FNR	ferredoxin:$NADP^+$ reductase

in situ,in vitro	in membrane, in solution
ISP	iron-sulfur protein
MOAS	β-methacrylate stilbene
NQNO	2*n*-nonyl-4-hydroxy-quinoline-*N*-oxide
PQ-9, UQ-10	plasto-, ubiquinone with 9, 10 isoprenoids
Q,QH_2	quinone, quinol
$Q^{\bullet-}$	semiquinone
RMSD	root mean square Q deviation
TMH	trans-membrane α-helix
UDM	undecyl-β-D-maltoside
UHDBT	5-undecyl-6-hydroxy-4,7-dioxobenzothiazole
$\Delta\tilde{\mu}H^+$	trans-membrane electrochemical proton gradient
V	volt

References

1. Berry EA, Huang L-S, Earnest TN, Jap BK. X-ray diffraction by crystals of beef heart ubiquinol:cytochrome *c* oxidoreductase. J Mol Biol. 1992; 224:1161–1166. [PubMed: 1314906]
2. Xia D, Yu CA, Deisenhofer J, Xia J-Z, Yu L. Three dimensional structure of beef-heart mitochondrial cytochrome bc_1 complex. Biophys J. 1996; 70:253a.
3. Xia D, Yu C-A, Kim H, Xia J-Z, Kachurin AM, Yu L, Deisenhofer J. Crystal structure of the cytochrome bc_1 complex from bovine heart mitochondria. Science (New York, NY. 1997; 277:60–66.
4. Iwata S, Lee JW, Okada K, Lee JK, Iwata M, Rasmussen B, Link TA, Ramaswamy S, Jap BK. Complete structure of the 11-subunit bovine mitochondrial cytochrome bc_1 complex. Science (New York, NY. 1998; 281:64–71.
5. Zhang Z, Huang L, Shulmeister VM, Chi YI, Kim KK, Hung LW, Crofts AR, Berry EA, Kim SH. Electron transfer by domain movement in cytochrome bc_1. Nature. 1998; 392:677–684. [PubMed: 9565029]
6. Berry EA, Huang LS, Zhang Z, Kim SH. Structure of the avian mitochondrial cytochrome bc_1 complex. J Bioenerg Biomem. 1999; 31:177–190.
7. Hunte C, Koepke J, Lange C, Rossmanith T, Michel H. Structure at 2.3 Å resolution of the cytochrome bc_1 complex from the yeast *Saccharomyces cerevisiae* with an antibody Fv fragment. Struct Fold Des. 2000; 8:669–684.
8. Gao X, Wen X, Yu C, Esser L, Tsao S, Quinn B, Zhang L, Yu L, Xia D. The crystal structure of mitochondrial cytochrome bc_1 in complex with famoxadone: The role of aromatic-aromatic interaction in inhibition. Biochemistry. 2002; 41:11692–11702. [PubMed: 12269811]
9. Lange C, Hunte C. Crystal structure of the yeast cytochrome bc_1 complex with its bound substrate cytochrome *c*. Proc Nat Acad Sci USA. 2002; 99:2800–2805. [PubMed: 11880631]
10. Gao X, Wen X, Esser L, Quinn B, Yu L, Yu C, Xia D. Structural basis for the quinone reduction in the bc_1 complex: A comparative analysis of crystal structure of mitochondrial cytochrome bc_1 with bound substrate and inhibitors at the Qi site. Biochemistry. 2003; 42:9067–9080. [PubMed: 12885240]
11. Palsdottir H, Lojero CG, Trumpower BL, Hunte C. Structure of the yeast cytochrome bc_1 complex with a hydroxyquinone anion Qo site inhibitor bound. J Biol Chem. 2003; 278:31303–31311. [PubMed: 12782631]

12. Esser L, Quinn B, Li YF, Zhang M, Elberry M, Yu L, Yu CA, Xia D. Crystallographic studies of quinol oxidation site inhibitors: a modified classification of inhibitors for the cytochrome bc_1 complex. J Mol Biol. 2004; 341:281–302. [PubMed: 15312779]
13. Esser L, Gong X, Yang S, Yu L, Yu CA, Xia D. Surface-modulated motion switch: capture and release of iron-sulfur protein in the cytochrome bc_1 complex. Proc Nat Acad Sci USA. 2006; 103:13045–13050. [PubMed: 16924113]
14. Esser L, Elberry M, Zhou F, Yu CA, Yu L, Xia D. Inhibitor-complexed structures of the cytochrome bc_1 from the photosynthetic bacterium *Rhodobacter sphaeroides*. Biol Chem. 2008; 283:2846–2857.
15. Solmaz SR, Hunte C. Structure of complex III with bound cytochrome *c* in reduced state and definition of a minimal core interface for electron transfer. J Biol Chem. 2008; 283:17542–17549. [PubMed: 18390544]
16. Kurisu G, Zhang H, Smith JL, Cramer WA. Structure of the cytochrome b_6f complex of oxygenic photosynthesis: tuning the cavity. Science (New York, NY. 2003; 302:1009–1014.
17. Stroebel D, Choquet Y, Popot JL, Picot D. An atypical heam in the cytochrome b_6f complex. Nature. 2003; 426:413–418. [PubMed: 14647374]
18. Yan J, Kurisu G, Cramer WA. Structure of the cytochrome b_6f complex: Binding site and intraprotein transfer of the quinone analogue inhibitor 2,5-dibromo-3-methyl-6-isopropyl-*p*-benzoquinone. Proc Nat Acad Sci USA. 2006; 103:67–74.
19. Yamashita E, Zhang H, Cramer WA. Structure of the cytochrome b_6f complex: quinone analogue inhibitors as ligands of heme c_n. J Mol Biol. 2007; 370:39–52. [PubMed: 17498743]
20. Baniulis D, Yamashita E, Whitelegge JP, Zatsman AI, Hendrich MP, Hasan SS, Ryan CM, Cramer WA. Structure-Function, Stability, and Chemical Modification of the Cyanobacterial Cytochrome b_6f Complex from Nostoc sp. CC 7120. J Biol Chem. 2009; 284:9861–9869. [PubMed: 19189962]
21. Iwata S, Saynovits M, Link TA, Michel H. Structure of a water-soluble fragment of the 'Rieske' iron-sulfur protein of the bovine heart mitochondrial cytochrome bc_1 complex determined by MAD phasing at 1.5 Å resolution. Structure. 1996; 4:567–579. [PubMed: 8736555]
22. Zhang H, Carrell CJ, Huang D, Sled V, Ohnishi T, Smith JL, Cramer WA. Characterization and Crystallization of the Lumen-Side Domain of the Chloroplast Rieske Iron-Sulfur Protein. J Biol Chem. 1996; 271:31360–31366. [PubMed: 8940143]
23. Carrell CJ, Zhang H, Cramer WA, Smith JL. Biological identity and diversity in photosynthesis and respiration: structure of the lumen-side domain of the chloroplast Rieske protein. Structure. 1997; 5:1613–1625. [PubMed: 9438861]
24. Hunsicker-Wang LM, Heine A, Chen Y, Luna EP, Todaro T, Zhang YM, Williams PA, McRee DE, Hirst J, Stout CD, Fee JA. High-resolution structure of the soluble, respiratory-type Rieske protein from Thermus thermophilus: analysis and comparison. Biochemistry. 2003; 42:7303–7317. [PubMed: 12809486]
25. Kolling DJ, Brunzelle JS, Lhee S, Crofts AR, Nair SK. Atomic resolution structures of Rieske iron-sulfur protein: role of hydrogen bonds in tuning the redox potential of iron-sulfur clusters. Structure. 2007; 15:29–38. [PubMed: 17223530]
26. Martinez, SE.; Smith, JL.; Huang, D.; Szczepaniak, A.; Cramer, WA. Crystallographic studies of the lumen-side domain of turnip cytochrome *f*. In: Murata, N., editor. Research in Photosynthesis. Kluwer Academic Publishers; Dordrecht: 1992. p. 495-498.
27. Martinez SE, Huang D, Szczepaniak A, Cramer WA, Smith JL. Crystal structure of the chloroplast cytochrome *f* reveals a novel cytochrome fold and unexpected heme ligation. Structure. 1994; 2:95–105. [PubMed: 8081747]
28. Martinez S, Huang D, Ponamarev M, Cramer WA, Smith JL. The heme redox center of chloroplast cytochrome *f* is linked to a buried five-water chain. Protein Sci. 1996; 5:1081–1092. [PubMed: 8762139]
29. Chi YI, Huang LS, Zhang Z, Fernandez-Velasco JG, Berry EA. X-ray structure of a truncated form of cytochrome *f* from *Chlamydomonas reinhardtii*. Biochemistry. 2000; 39:7689–7701. [PubMed: 10869174]

30. Sainz G, Carrell CJ, Ponamarev MV, Soriano GM, Cramer WA, Smith JL. Interruption of the internal water chain of cytochrome *f* impairs photosynthetic function. Biochemistry. 2000; 39:9164–9173. [PubMed: 10924110]
31. Widger WR, Cramer WA, Herrmann RG, Trebst A. Sequence homology and structural similarity between the *b* cytochrome of mitochondrial complex III and the chloroplast b_6f complex: position of the cytochrome *b* hemes in the membrane. Proc Natl Acad Sci, U S A. 1984; 81:674–678. [PubMed: 6322162]
32. Furbacher, PN.; Tae, G-S.; Cramer, WA. Evolution and origins of cytochrome bc_1 and b_6f complexes. In: Baltscheffsky, H., editor. Origin and Evolution of Biological Energy Conversion. VCH Publishers; New York: 1996. p. 221-253.
33. Schutz M, Brugna M, Lebrun E, Baymann F, Huber R, Stetter KO, Hauska G, Toci R, Lemesle-Meunier D, Tron P, Schmidt C, Nitschke W. Early evolution of cytochrome *bc* complexes. J Mol Biol. 2000; 300:663–675. [PubMed: 10891261]
34. Baymann F, Lebrun E, Brugna M, Schoepp-Cothenet B, Giudici-Orticoni MT, Nitschke W. The redox protein construction kit: pre-last universal common ancestor evolution of energy-conserving enzymes. Philos Trans Royal Soc Lond B Biol Sci. 2003; 358:267–274.
35. Mulkidjanian A, Koonin E, Makarova K, Haselkorn R, Galperin M. The cyanobacterial genome core and the origin of photosynthesis. Photosyn Res. 2007; 91:269–269.
36. Baymann, F.; Nitschke, W. Photosyn Res. Vol. 104. 2010. Heliobacterial Rieske/cyt *b* complex; p. 177-187.
37. Nitschke W, van Lis R, Schoepp-Cothenet B, Baymann F. The “green” phylogenetic clade of Rieske/cyt *b* complexes. Photosyn Res. 2010; 104:347–355. [PubMed: 20130997]
38. Crofts AR, Wang Z. How rapid are the internal reactions of the ubiquinol: cytochrome c_2 oxidoreductase? Photosynthesis research. 1989; 22:69–87.
39. Brandt U, Trumpower B. The protonmotive Q cycle in mitochondria and bacteria. Crit Rev Biochem Mol Biol. 1994; 29:165–197. [PubMed: 8070276]
40. Crofts AR, Berry EA. Structure and function of the cytochrome bc_1 complex of mitochondria and photosynthetic bacteria. Curr Op Struct Biol. 1998; 8:501–509.
41. Smith JL. Secret life of cytochrome bc_1. Science (New York, NY. 1998; 281:58–59.
42. Berry E, Guergova-Kuras M, Huang L-S, Crofts AR. Structure and function of cytochrome *bc* complexes. Ann Rev Biochem. 2000; 69:1005–1075. [PubMed: 10966481]
43. Darrouzet E, Moser CC, Dutton PL, Daldal F. Large scale domain movement in cytochrome bc(1): a new device for electron transfer in proteins. Trends Biochem Sci. 2001; 26:445–451. [PubMed: 11440857]
44. Hunte C. Insights from the structure of the yeast cytochrome bc1 complex: crystallization of membrane proteins with antibody fragments. FEBS Lett. 2001; 504:126–132. [PubMed: 11532444]
45. Trumpower BL. A concerted, alternating sites mechanism of ubiquinol oxidation by the dimeric cytochrome bc_1 complex. Biochim Biophys Acta. 2002; 1555:166–173. [PubMed: 12206910]
46. Hunte C, Palsdottir H, Trumpower BL. Protonmotive pathways and mechanisms in the cytochrome bc_1 complex. FEBS Lett. 2003; 545:39–46. [PubMed: 12788490]
47. Crofts AR. The Q-cycle - A Personal Perspective. Photosynth Res. 2004; 80:223–243. [PubMed: 16328823]
48. Crofts AR. The cytochrome bc_1 complex: Function in the context of structure. Ann Rev Physiol. 2004; 66:689–733. [PubMed: 14977419]
49. Osyczka A, Moser CC, Dutton PL. Reversible redox energy coupling in electron transfer chains. Nature. 2004; 427:607–612. [PubMed: 14961113]
50. Palsdottir H, Hunte C. Lipids in membrane protein structures. Biochim Biophys Acta. 2004; 1666:2–18. [PubMed: 15519305]
51. Mulkidjanian AY. Ubiquinol oxidation in the cytochrome bc_1 complex: Reaction mechanism and prevention of short-circuiting. Biochim Biophys Acta. 2005; 1709:5–34. [PubMed: 16005845]
52. Osyczka A, Moser CC, Dutton PL. Fixing the Q cycle. Trends Biochem Sci. 2005; 30:176–182. [PubMed: 15817393]

53. Mulkidjanian AY. Proton translocation by the cytochrome bc_1 complexes of phototrophic bacteria: introducing the activated Q-cycle. Photochem Photobiol Sci. 2007; 6:19–34. [PubMed: 17200733]
54. Wenz T, Covian R, Hellwig P, Macmillan F, Meunier B, Trumpower BL, Hunte C. Mutational analysis of cytochrome *b* at the ubiquinol oxidation site of yeast complex III. J Biol Chem. 2007; 282:3977–3988. [PubMed: 17145759]
55. Xia D, Esser L, Yu L, Yu CA. Structural basis for the mechanism of electron bifurcation at the quinol oxidation site of the cytochrome bc1 complex. Photosynthesis research. 2007; 92:17–34. [PubMed: 17457691]
56. Covian R, Trumpower BL. The dimeric structure of the cytochrome bc_1 complex prevents center P inhibition by reverse reactions at center N. Biochim Biophys Acta. 2008; 1777:1044–1052. [PubMed: 18454936]
57. Covian R, Trumpower BL. Regulatory interactions in the dimeric cytochrome bc_1 complex: the advantages of being a twin. Biochim Biophys Acta. 2008; 1777:1079–10791. [PubMed: 18471987]
58. Crofts AR, Holland JT, Victoria D, Kolling DR, Dikanov SA, Gilbreth R, Lhee S, Kuras R, Kuras MG. The Q-cycle reviewed: How well does a monomeric mechanism of the bc_1 complex account for the function of a dimeric complex? Biochim Biophys Acta. 2008; 1777:1001–1019. [PubMed: 18501698]
59. Hunte C, Richers S. Lipids and membrane protein structures. Curr Opin Struct Biol. 2008; 18:406–411. [PubMed: 18495472]
60. Hunte C, Solmaz S, Palsdottir H, Wenz T. A structural perspective on mechanism and function of the cytochrome bc (1) complex. Results Probl Cell Differ. 2008; 45:253–278. [PubMed: 18038116]
61. Ransac S, Parisey N, Mazat JP. The loneliness of the electrons in the bc_1 complex. Biochim Biophys Acta. 2008; 1777:1053–1059. [PubMed: 18534187]
62. Wenz T, Hielscher R, Hellwig P, Schagger H, Richers S, Hunte C. Role of phospholipids in respiratory cytochrome bc_1 complex catalysis and supercomplex formation. Biochim Biophys Acta. 2009; 1787:609–616. [PubMed: 19254687]
63. Castellani R, Covian R, Kleinschroth T, Anderka O, Ludwig B, Trumpower BL. Direct demonstration of half-of-the-sites reactivity in the dimeric cytochrome bc_1 complex. J Biol Chem. 2010; 285:507–510.
64. Cooley JW. A structural model for across membrane coupling between the Q_o and Q_i active sites of cytochrome bc_1. Biochim Biophys Acta. 2010
65. Hope AB. The chloroplast cytochrome *bf* complex: A critical focus on function. Biochim Biophys Acta. 1993; 1143:1–22. [PubMed: 8388722]
66. Kallas, T. The cytochrome b_6f complex. In: Bryant, DA., editor. The Molecular Biology of Cyanobacteria. Kluwer Academic Publishers; Dordrecht: 1994. p. 259-317.
67. Hauska, G.; Schütz, M.; Büttner, M. The cytochrome b_6f complex-composition, structure, and function. In: Ort, DR.; Yocum, CF., editors. Oxygenic photosynthesis: The light reactions. Kluwer Academic Publisher; Amsterdam: 1996.
68. Allen JF. Cytochrome b_6f: structure for signaling and vectorial metabolism. Trends Plant Sci. 2004; 9:130–137. [PubMed: 15003236]
69. Cramer WA, Zhang H, Yan J, Kurisu G, Smith JL. Evolution of photosynthesis: time-independent structure of the cytochrome b_6f complex. Biochemistry. 2004; 43:5921–5929. [PubMed: 15147175]
70. Cramer WA, Yan J, Zhang H, Kurisu G, Smith JL. Structure of the cytochrome b_6f complex: new prosthetic groups, Q-space, and the 'hors d'oeuvres hypothesis' for assembly of the complex. Photosynth Res. 2005; 85:133–143. [PubMed: 15977064]
71. Cramer WA, Zhang H. Consequences of the structure of the cytochrome b_6f complex for its charge transfer pathways. Biochim Biophys Acta. 2006; 1757:339–345. [PubMed: 16787635]
72. Cramer WA, Zhang H, Yan J, Kurisu G, Smith JL. Trans-membrane traffic in the cytochrome b_6f complex. Ann Rev Biochem. 2006; 75:769–790. [PubMed: 16756511]
73. Baniulis D, Yamashita E, Zhang H, Hasan SS, Cramer WA. Structure-function of the cytochrome b_6f complex. Photochem Photobiol Sci. 2008; 84:1349–1358.

74. Cramer, WA.; Baniulis, D.; Yamashita, E.; Zhang, H.; Zatsman, AI.; Hendrich, MP. Structure, spectroscopy, and function of the cytochrome b_6f complex: heme c_n and n-side electron and proton transfer reactions. In: Fromme, P., editor. Photosynthetic Protein Complexes: a Structural Approach. Wiley-VCH; Weinheim: 2008. p. 155-179.
75. Cramer, WA.; Zhang, H.; Yan, J.; Kurisu, G.; Yamashita, E.; Dashdorj, N.; Kim, H.; Savikhin, S. Structure-function of the cytochrome b_6f complex: a design that has worked for three billion years. In: Renger, G., editor. Comprehensive Series in Photochemistry and Photobiology. Royal Soc. of Chemistry; Cambridge: 2008. p. 417-446.
76. Cramer, WA.; Yamashita, E.; Baniulis, D.; Hasan, SS. The cytochrome b_6f complex of oxygenic photosynthesis. In: Messerschmidt, A., editor. Handbook of Metalloproteins. John Wiley; Chichester: 2010.
77. Nowaczyk MM, Sander J, Grasse N, Cormann KU, Rexroth D, Bernat G, Rogner M. Dynamics of the cyanobacterial photosynthetic network: Communication and modification of membrane protein complexes. Eur J Cell Biol. 2010
78. Soriano GM, Ponamarev MV, Carrell CJ, Xia D, Smith JL, Cramer WA. Comparison of the cytochrome bc_1 complex with the anticipated structure of the cytochrome b_6f complex: Le plus ca change le plus c'est la meme chose. J Bioenerg Biomembr. 1999; 31:201–213. [PubMed: 10591526]
79. Cape JL, Bowman MK, Kramer DM. Understanding the cytochrome *bc* complexes by what they don't do. The Q-cycle at 30. Trends Plant Sci. 2006; 11:46–55. [PubMed: 16352458]
80. Mulkidjanian AY. Activated Q cycle as a common mechanism for cytochrome bc_1 and b_6f complexes. Biochim Biophys Acta. 2010; 1797:1858–1868. [PubMed: 20650262]
81. Swierczek M, Cieluch E, Sarewicz M, Borek A, Moser CC, Dutton PL, Osyczka A. An electronic bus bar lies in the core of cytochrome bc_1. Science (New York, NY). 2010; 329:451–454.
82. Covian R, Zwicker K, Rotsaert FA, Trumpower BL. Asymmetric and redox-specific binding of quinone and quinol at center N of the dimeric yeast cytochrome bc_1 complex. Consequences for semiquinone stabilization. J Biol Chem. 2007; 282:24198–24208. [PubMed: 17584742]
83. Hosler JP, Yocum CF. Regulation of cyclic photophosphorylation during ferredoxin-mediated electron transport : effect of DCMU and the NADPH/NADP ratio. Plant Physiol. 1987; 83:965–969. [PubMed: 16665372]
84. Heber U. Irrungen, Wirrungen? The Mehler reaction in relation to cyclic electron transport in C3 plants. Photosynth Res. 2002; 73:223–231. [PubMed: 16245125]
85. Finazzi G, Forti G. Metabolic flexibility of the green alga Chlamydomonas reinhardtii as revealed by the link between state transitions and cyclic electron flow. Photosyn Res. 2004; 82:327–338. [PubMed: 16143844]
86. Golding AJ, Finazzi G, Johnson GN. Reduction of the thylakoid electron transport chain by stromal reductants--evidence for activation of cyclic electron transport upon dark adaptation or under drought. Planta. 2004; 220:356–363. [PubMed: 15316779]
87. Johnson GN. Cyclic electron transport in C3 plants: fact or artefact? J Exper Botany. 2005; 56:407–416. [PubMed: 15647314]
88. Joliot P, Joliot A. Quantification of cyclic and linear flows in plants. Proc Nat Acad Sci USA. 2005; 102:4913–4918. [PubMed: 15781857]
89. Breyton C, Nandha B, Johnson GN, Joliot P, Finazzi G. Redox modulation of cyclic electron flow around photosystem I in C3 plants. Biochemistry. 2006; 45:13465–13475. [PubMed: 17087500]
90. Joliot P, Joliot A. Cyclic electron flow in C3 plants. Biochim Biophys Acta. 2006; 1757:362–368. [PubMed: 16762315]
91. Nelson N, Yocum CF. Structure and function of photosystems I and II. Ann Rev Plant Biol. 2006; 57:521–565. [PubMed: 16669773]
92. Nandha B, Finazzi G, Joliot P, Hald S, Johnson GN. The role of PGR5 in the redox poising of photosynthetic electron transport. Biochim Biophys Acta. 2007; 1767:1252–1259. [PubMed: 17803955]
93. Shikanai T. Cyclic electron transport around photosystem I: genetic approaches. Ann Rev Plant Biol. 2007; 58:199–217. [PubMed: 17201689]

94. DalCorso G, Pesaresi P, Masiero S, Aseeva E, Schunemann D, Finazzi G, Joliot P, Barbato R, Leister D. A complex containing PGRL1 and PGR5 is involved in the switch between linear and cyclic electron flow in Arabidopsis. Cell. 2008; 132:273–285. [PubMed: 18243102]

95. Alric J, Lavergne J, Rappaport F. Redox and ATP control of photosynthetic cyclic electron flow in *Chlamydomonas reinhardtii* (I) aerobic conditions. Biochim Biophys Acta. 2010; 1797:44–51. [PubMed: 19651104]

96. Iwai M, Takizawa K, Tokutsu R, Okamuro A, Takahashi Y, MInagawa J. Isolation of the supercomplex that drives cyclic electron flow in photosynthesis. Nature. 2010; 464:1210–1213. [PubMed: 20364124]

97. Livingston AK, Cruz JA, Kohzuma K, Dhingra A, Kramer DM. An Arabidopsis mutant with high cyclic electron flow around photosystem I (hcef) involving the NADPH dehydrogenase complex. Plant Cell. 2010; 22:221–233. [PubMed: 20081115]

98. Livingston A, Kanazawa A, Cruz JA, Kramer DM. Regulation of cyclic electron flow in C(3) plants: differential effects of limiting photosynthesis at ribulose-1,5-bisphosphate carboxylase/oxygenase and glyceraldehyde-3-phosphate dehydrogenase. Plant Cell Envir. 2010

99. Okegawa Y, Kobayashi Y, Shikanai T. Physiological links among alternative electron transport pathways that reduce and oxidize plastoquinone in Arabidopsis. Plant J. 2010; 63:458–468.

100. Chance B, Williams GB. The respiratory chain and oxidative phosphorylation. Adv Enzymol. 1956; 17:65–135.

101. Tagawa K, Tsujimoto HY, Arnon DL. Role of chloroplast ferredoxin in the energy conversion process of photosynthesis. Biochemistry. 1963; 49:567–572.

102. Moss DA, Bendall DS. Cyclic electron transport in chloroplasts. the Q-cycle and the site of action of antimycin. Biochim Biophys Acta. 1984; 767:389–395.

103. Slovacek RE, Crowther D, Hind G. Cytochrome function in the cyclic electron transport pathway of chloroplasts. Biochim Biophys Acta. 1979; 547:138–148. [PubMed: 465483]

104. Lavergne J. Membrane potential-dependent reduction of cytochrome b_6 in an algal mutant lacking photosystem I centers. Biochim Biophys Acta. 1983; 725:25–33.

105. Joliot P, Joliot A. The low-potential electron-transfer chain in the cytochrome *bf* complex. Biochim Biophys Acta. 1988; 933:319–333.

106. Zhang H, Whitelegge JP, Cramer WA. Ferredoxin: $NADP^+$ oxidoreductase is a subunit of the chloroplast cytochrome b_6f complex. J Biol Chem. 2001; 276:38159–38165. [PubMed: 11483610]

107. Girvin, ME. Ph D Thesis. Purdue University; 1985. Electron and proton transfer in the quinone-cytochrome *bf* region of chloroplasts.

108. Fato R, Battino M, Degli Esposti M, Parenti Castelli G, Lenaz G. Determination of partition and lateral diffusion coefficients of ubiquinones by fluorescence quenching of n-(9-anthroyloxy)stearic acids in phospholipid vesicles and mitochondrial membranes. Biochemistry. 1986; 25:3378–3390. [PubMed: 3730366]

109. Wikström M, Krab K. The semiquinone cycle. A hypothesis of electron transfer and proton translocation in cytochrome *bc*-type complexes. J Bioenerg Biomem. 1986; 18:181–193.

110. Blackwell MF, Whitmarsh J. Effect of integral membrane proteins on the lateral mobility of plastoquinone in phosphatidylcholine proteoliposomes. Biophys J. 1990; 58:1259–1271. [PubMed: 19431774]

111. Joliot P, Joliot A. Mechanism of electron transfer in the cytochrome *bf* complex of algae: evidence for a semiquinone cycle. Proc Nat Acad Sci USA. 1994; 91:1034–1038. [PubMed: 11607457]

112. Shiver JW, Peterson AA, Widger WR, Furbacher PN, Cramer WA. Prediction of bilayer spanning domains of hydrophobic and amphipathic membrane proteins: application to the cytochrome *b* and colicin families. Meth Enzymol. 1989; 172:439–461. [PubMed: 2747538]

113. Saraste M. Location of haem-binding sites in the mitochondrial cytochrome *b*. EBS Lett. 1984; 166:367–372.

114. Crofts, AR.; Robinson, H.; Andrews, K.; van Doren, S.; Berry, E. Catalytic sites for reduction and oxidation of quinones. In: Papa, S.; Chance, B.; Ernster, L., editors. International Workshop of

Cytochrome Systems: Molecular Biology and Bioenergetics. Plenum Press; Bari, Italy: 1987. p. 617-624.

115. Degli Esposti M, De Vries S, Crimi M, Ghelli A, Patarnello T, Meyer A. Mitochondrial cytochrome *b*: evolution and structure of the protein. Biochim Biophys Acta. 1993; 1143:243–271. [PubMed: 8329437]
116. Rieske JS, Zaugg WS, Hansen RE. Studies on the Electron Transfer System. Lix. Distribution of Iron and of the Component Giving an Electron Paramagnetic Resonance Signal at G = 1.90 in Subfractions of Complex 3. J Biol Chem. 1964; 239:3023–3030. [PubMed: 14217891]
117. Cooley, JW.; Nitschke, W.; Kramer, DM. The cytochrome bc1 and related bc complexes, the Rieske/cytochrome b complex as the functional core of a central electron/proton transfer complex. In: Hunter, CN.; Daldal, F.; Thurnauer, M.; Beatty, JT., editors. The Purple Photosynthetic Bacteria. Springer-Verlag; Dordrecht: 2008. p. 451-473.
118. Bonisch H, Schmidt CL, Schafer G, Ladenstein R. The structure of the soluble domain of an archaeal Rieske iron-sulfur protein at 1.1 Å resolution. J Mol Biol. 2002; 319:791–805. [PubMed: 12054871]
119. Lebrun E, Santini JM, Brugna M, Ducluzeau AL, Ouchane S, Schoepp-Cothenet B, Baymann F, Nitschke W. The Rieske protein: a case study on the pitfalls of multiple sequence alignments and phylogenetic reconstruction. Mol Biol Evol. 2006; 23:1180–1191. [PubMed: 16569761]
120. Lancaster CRD, Kroeger A, Auer M, Michel M. Structure of fumarate reductase from Wollinella succinogenes at 2.2 A resolution. Nature. 1999; 402:377–385. [PubMed: 10586875]
121. Jormakka M, Toernroth S, Byrne B, Iwata S. Molecular basis of proton motive force generation: structure of formate dehydrogenase-N. Science (New York) NY. 2002; 295:1863–1868.
122. Tsukihara T, Aoyama H, Yamashita E, Tomizaki T, Yamaguchi H, Shinzawa-Itono K, Nakashima R, Yaono R, Yoshikawa S. The whole structure of the 13-subunit oxidized cytochrome *c* oxidase at 2.8 Å. Science (New York, NY. 1996; 272:1136–1144.
123. Ostermeier C, Harrenga A, Ermler U, Michel H. Structure at 2.7 angstrom resolution of the Paracoccus denitrificans two subunit cytochrome c oxidase complexed with an antibody Fv fragment. Proc Natl Acad Sci, U S A. 1997; 94:10547–10553. [PubMed: 9380672]
124. Svensson-Ek M, Abramson J, Larsson G, Toernroth P. Structure of cytochrome c oxidase from Rhodobacter sphaeroides. J Mol Biol. 2002; 321:329–339. [PubMed: 12144789]
125. Qin L, Hiser C, Mulichak A, Garavito RM, Ferguson-Miller S. Identification of conseved lipid/detergent binding site in a high resolution structure of the memebrane protein, Cytochrome c oxidase. Proc Natl Acad Sci USA. 2006; 103:16117–16122. [PubMed: 17050688]
126. Berry EA, Walker FA. Bis-histidine-coordinated hemes in four-helix bundles: how the geometry of the bundle controls the axial imidazole plane orientations in transmembrane cytochromes of mitochondrial complexes II and III and related proteins. J Biol Inorg Chem. 2008; 13:481–498. [PubMed: 18418633]
127. Zatsman AI, Zhang H, Gunderson WA, Cramer WA, Hendrich MP. Heme-heme interactions in the cytochrome b_6f complex: EPR spectroscopy and correlation with structure. J Amer Chem Soc. 2006; 128:14246–14247. [PubMed: 17076484]
128. Baymann F, Giusti F, Picot D, Nitschke W. The ci/bH moiety in the b_6f complex studied by EPR: a pair of strongly interacting hemes. Proc Nat Acad Sci USA. 2007; 104:519–524. [PubMed: 17202266]
129. Twigg AI, Baniulis D, Cramer WA, Hendrich MP. EPR detection of an O_2 surrogate bound to heme c_n of the cytochrome b_6f complex. J Am Chem Soc. 2009; 131:12536–12537. [PubMed: 19689132]
130. Alric J, Pierre Y, Picot D, Lavergne J, Rappaport F. Spectral and redox characterization of the heme c_i of the cytochrome b_6f complex. Proc Nat Acad Sci USA. 2005; 102:15860–15865. [PubMed: 16247018]
131. Kuras R, Saint-Marcoux D, Wollman FA, de Vitry C. A specific *c*-type cytochrome maturation system is required for oxygenic photosynthesis. Proc Nat Acad Sci USA. 2007; 104:9906–9910. [PubMed: 17535914]
132. Saint-Marcoux D, Wollman FA, de Vitry C. Biogenesis of cytochrome b_6 in photosynthetic membranes. J Cell Biol. 2009; 185:1195–1207. [PubMed: 19564403]

133. Malnoë A, Girard-Bascou J, Baymann F, Alric J, Rappaport F, Wollman FA, de Vitry C. Photosynthesis with simplified cytochrome b_6f complexes: Are all hemes required? Biochim Biophys Acta. 2010; 1797:19.

134. Huang D, Everly RM, Cheng RH, Heymann JB, Schägger H, Sled V, Ohnishi T, Baker TS, Cramer WA. Characterization of the chloroplast cytochrome b_6f complex as a structural and functional dimer. Biochemistry. 1994; 33:4401–4409. [PubMed: 8155658]

135. Pierre Y, Breyton C, Lemoine Y, Robert B, Vernotte C, Popot J-L. On the presence and role of a molecule of chlorophyll a in the cytochrome b_6f complex. J Biol Chem. 1997; 272:21901–21908. [PubMed: 9268323]

136. Zhang H, Huang D, Cramer WA. Stoichiometrically bound beta-carotene in the cytochrome b_6f complex of oxygenic photosynthesis protects against oxygen damage. J Biol Chem. 1999; 274:1581–1587. [PubMed: 9880536]

137. Clark RD, Hawkesford MJ, Coughlan SJ, Hind G. Association of ferredoxin-$NADP^+$ oxidoreductase with the chloroplast cytochrome *bf* complex. EBS Lett. 1984; 174:137–142.

138. Coughlan S, Matthijs HC, Hind G. The ferredoxin-$NADP^+$ oxidoreductase-binding protein is not the 17-kDa component of the cytochrome *b/f* complex. J Biol Chem. 1985; 260:14891–14893. [PubMed: 3905786]

139. Volkmer T, Schneider D, Bernat G, Kirchhoff H, Wenk SO, Rogner M. Ssr2998 of *Synechocystis* sp. PCC 6803 is involved in regulation of cyanobacterial electron transport and associated with the cytochrome b_6f complex. J Biol Chem. 2007; 282:3730–3737. [PubMed: 17166849]

140. Depege N, Bellafiore S, Rochaix JD. Role of chloroplast protein kinase Stt7 in LHCII phosphorylation and state transition in Chlamydomonas. Science (New York, NY. 2003; 299:1572–1575.

141. Vener AV, van Kan PJ, Rich PR, Ohad I, Andersson B. Plastoquinol at the quinol oxidation site of reduced cytochrome bf mediates signal transduction between light and protein phosphorylation: thylakoid protein kinase deactivation by a single-turnover flash. Proceedings of the National Academy of Sciences of the United States of America. 1997; 94:1585–1590. [PubMed: 11038603]

142. Zito F, Finazzi G, Delosme R, Nitschke W, Picot D, Wollman FA. The Qo site of cytochrome b(6)f complexes controls the activation of the LHCII kinase. EMBO Journal. 1999; 18:2961–2969. [PubMed: 10357809]

143. Allen JF. Protein phosphorylation in regulation of photosynthesis. Biochim Biophys Acta. 1992; 1098:275–335. [PubMed: 1310622]

144. Hamel P, Olive J, Pierre Y, Wollman FA, de Vitry C. A new subunit of cytochrome b_6f complex undergoes reversible phosphorylation upon state transition. J Biol Chem. 2000; 275:17072–17079. [PubMed: 10748028]

145. Smirnova I, Kasho V, Sugihara J, Kaback HR. Probing of the rates of alternating access in LacY with Trp fluorescence. Proc Nat Acad Sci USA. 2009; 106:21561–21566. [PubMed: 19959662]

146. Huang Y, Lemieux MJ, Song J, Auer M, Wang DN. Structure and mechanism of the glycerol-3-phosphate transporter from *Escherichia coli*. Science (New York, NY. 2003; 301:616–620.

147. Lange C, Nett JH, Trumpower BL, Hunte C. Specific roles of protein-phospholipid interactions in the yeast cytochrome bc1 complex structure. EMBO J. 2001; 20:6591–6600. [PubMed: 11726495]

148. Pfeiffer K, Gohil V, Stuart RA, Hunte C, Brandt U, Greenberg ML, Schagger H. Cardiolipin stabilizes respiratory chain supercomplexes. The Journal of biological chemistry. 2003; 278:52873–52880. [PubMed: 14561769]

149. Hielscher R, Wenz T, Hunte C, Hellwig P. Monitoring the redox and protonation dependent contributions of cardiolipin in electrochemically induced FTIR difference spectra of the cytochrome bc(1) complex from yeast. Biochim Biophys Acta. 2009; 1787:617–625. [PubMed: 19413949]

150. Pomes R, Roux B. Structure and dynamics of a proton wire: a theoretical study of H+ translocation along the single-file water chain in the gramicidin A channel. Biophysical journal. 1996; 71:19–39. [PubMed: 8804586]

151. de Vitry C, Ouyang Y, Finazzi G, Wollman FA, Kallas T. The chloroplast Rieske iron-sulfur protein. At the crossroad of electron transport and signal transduction. J Biol Chem. 2004; 279:44621–44627. [PubMed: 15316016]
152. Zhang H, Kurisu G, Smith JL, Cramer WA. A defined protein-detergent-lipid complex for crystallization of integral membrane proteins: The cytochrome b_6f complex of oxygenic photosynthesis. Proc Nat Acad Sci USA. 2003; 100:5160–5163. [PubMed: 12702760]
153. Graan T, Ort DR. Quantitation of 2,5-dibromo-3-methyl-6-isopropyl-p-benzoquinone binding sites in chloroplast membranes: evidence for a functional dimer of the cytochrome b6f complex. Arch Biochem Biophys. 1986; 248:445–451. [PubMed: 3740838]
154. Covian R, Gutierrez-Cirlos EB, Trumpower BL. Anti-cooperative oxidation of ubiquinol by the yeast cytochrome bc_1 complex. J Biol Chem. 2004; 279:15040–15049. [PubMed: 14761953]
155. Moser CC, Keske JM, Warncke K, Farid RS, Dutton PL. Nature of biological electron transfer. Nature. 1992; 355:796–802. [PubMed: 1311417]
156. Iwata M, Bjorkman J, Iwata S. Conformational change of the Rieske [2Fe-2S] protein in cytochrome bc1 complex. J Bioenerg Biomembr. 1999; 31:169–175. [PubMed: 10591523]
157. Tian H, White S, Yu L, Yu C. Evidence for the head domain movement of the Rieske iron-sulfur protein in electron transfer reaction of the cytochrome bc_1 complex. J Biol Chem. 1999; 274:7146–7152. [PubMed: 10066773]
158. Darrouzet E, Valkova-Valchanova M, Moser CC, Dutton PL, Daldal F. Uncovering the [2Fe2S] domain movement in cytochrome bc1 and its implications for energy conversion. Proceedings of the National Academy of Sciences of the United States of America. 2000; 97:4567–4572. [PubMed: 10781061]
159. Nett JH, Hunte C, Trumpower BL. Changes to the length of the flexible linker region of the Rieske protein impair the interaction of ubiquinol with the cytochrome bc_1 complex. Euro J Biochem. 2000; 267:5777–5782.
160. Yan J, Cramer WA. Functional insensitivity of the cytochrome b_6f complex to structure changes in the hinge region of the Rieske iron-sulfur protein. The Journal of biological chemistry. 2003; 278:20925–20933. [PubMed: 12672829]
161. Brugna M, Rodgers S, Schricker A, Montoya G, Kazmeier M, Nitschke W, Sinning I. A spectroscopic method for observing the domain movement of the Rieske iron-sulfur protein. Proceedings of the National Academy of Sciences of the United States of America. 2000; 97:2069–2074. [PubMed: 10681446]
162. Breyton C. Conformational changes in the cytochrome b6f complex induced by inhibitor binding. The Journal of biological chemistry. 2000; 275:13195–13201. [PubMed: 10788423]
163. Rieske JS. Changes in oxidation-reduction potential of cytochrome *b* observed in the presence of antimycin A. Arch Biochem Biophys. 1971; 145:179–193. [PubMed: 5123136]
164. Cooley JW, Ohnishi T, Daldal F. Binding dynamics at the quinone reduction Q_i site influence the equilibrium interactions of the iron sulfur protein and hydroquinone oxidation Q_o site of the cytochrome bc_1 complex. Biochemistry. 2005; 44:10520–10532. [PubMed: 16060661]
165. Cooley JW, Lee DW, Daldal F. Across membrane communication between the Q_o and Q_i active sites of cytochrome bc_1. Biochemistry. 2009; 48:1888–1899. [PubMed: 19254042]
166. Crane FL, Hatefi Y, Lester RL, Widmer C. Isolation of a quinone from beef heart mitochondria. Biochim Biophys Acta. 1957; 25:220–221. [PubMed: 13445756]
167. Crane FL. Discovery of ubiquinone (coenzyme Q) and an overview of function. Mitochondrion. 2007; 7(Suppl):S2–7. [PubMed: 17446142]
168. Lenaz G. Lipid fluidity and membrane protein dynamics. Biosci Rep. 1987; 7:823–837. [PubMed: 3329533]
169. Di Bernardo S, Fato R, Casadio R, Fariselli P, Lenaz G. A high diffusion coefficient for coenzyme Q_{10} might be related to a folded structure. FEBS Lett. 1998; 426:77–80. [PubMed: 9598982]
170. Huang H, Hasan SS, Cramer WA, Post C. unpublished data. 2010
171. Wikström MKF, Berden JA. Oxido-reduction of cytochrome *b* in the presence of antimycin. Biochim Biophys Acta. 1972; 283:403–420. [PubMed: 4346389]

172. Mitchell P. The protonmotive Q cycle: A general formulation. FEBS Lett. 1975; 59:137–139. [PubMed: 1227927]
173. Mitchell P. Protonmotive redox mechanism of the cytochrome b-c1 complex in the respiratory chain: protonmotive ubiquinone cycle. FEBS Lett. 1975; 56:1–6. [PubMed: 239860]
174. Mitchell P. Possible molecular mechanisms of the protonmotive function of cytochrome systems. J Theor Biol. 1976; 62:327–367. [PubMed: 186667]
175. Rich PR, Wikström M. Evidence for a mobile semiquinone in the redox cycle of the mammalian cytochrome bc_1 complex. FEBS Lett. 1986; 194:176–181. [PubMed: 3000823]
176. Trumpower BL, Gennis RB. Energy transduction by cytochrome complexes in mitochondrial and bacterial respiration: the enzymology of coupling electron transfer reactions to transmembrane proton translocation. Ann Rev Biochem. 1994; 63:675–716. [PubMed: 7979252]
177. Gopta OA, Feniouk BA, Junge W, Mulkidjanian AY. The cytochrome bc_1 complex of *Rhodobacter capsulatus*: ubiquinol oxidation in a dimeric Q-cycle? FEBS Lett. 1998; 431:291–296. [PubMed: 9708922]
178. Trumpower BL. Function of the iron-sulfur protein of the cytochrome bc_1 segment in electron-transfer and energy-conserving reactions of the mitochondrial respiratory chain. Biochim Biophys Acta. 1981; 639:129–155. [PubMed: 6272847]
179. Prince RC, Matsuura K, Hurt E, Hauska G, Dutton PL. Reduction of cytocchrome b_6 and *f* in isolated plastoquinol-plastocyanin oxidoreductase driven by photochemical reaction centers from *Rhodopseudomonas sphaeroides*. J Biol Chem. 1982; 257:3379–3381. [PubMed: 7037783]
180. Leung KH, Hinkle PC. Reconstitution of Ion-Transport and Respiratory Control in Vesicles Formed from Reduced Coenzyme Q Cytochrome-C Reductase and Phospholipids. J Biol Chem. 1975; 250:8467–8471. [PubMed: 385]
181. Yang XH, Trumpower BL. Protonmotive Q cycle pathway of electron transfer and energy transduction in the three-subunit ubiquinol-cytochrome *c* oxidoreductase complex of *Paracoccus denitrificans*. J Biol Chem. 1988; 263:11962–11970. [PubMed: 2841340]
182. Hurt EC, Gabellini N, Shahak Y, Lockau W, Hauska G. Extra Proton Translocation and Membrane-Potential Generation Universal Properties of Cytochrome bc_1/b_6f Complexes Reconstituted into Liposomes. Arch Biochem Biophys. 1983; 225:879–885. [PubMed: 6312896]
183. Fowler CF, Kok B. Determination of H^+/e^- ratios in chloroplasts with flashing light. Biochim Biophys Acta. 1976; 423:510–523. [PubMed: 4099]
184. Berry S, Rumberg B. Proton to electron stoichiometry in electron transport of spinach thylakoids. Biochim Biophys Acta. 1999; 1410:248–261. [PubMed: 10082791]
185. Graan T, Ort DR. Initial events in the regulation of electron transfer in chloroplasts. J Biol Chem. 1983; 258:2831–2836. [PubMed: 6826542]
186. Sacksteder CA, Kanazawa A, Jacoby ME, Kramer DM. The proton to electron stoichiometry of steady-state photosynthesis in living plants: A proton-pumping Q cycle is continuously engaged. Proc Nat Acad Sci USA. 2000; 97:14283–14288. [PubMed: 11121034]
187. Girvin ME, Cramer WA. A redox study of the electron transport pathway responsible for generation of the slow electrochromic phase in chloroplasts. Biochim Biophys Acta. 1984; 767:29–38. [PubMed: 6487614]
188. Mulkidjanian AY, Junge W. Calibration and time resolution of lumenal pH-transients in chromatophores of *Rhodobacter capsulatus* following a single turnover flash of light: proton release by the cytochrome bc_1 complex is strongly electrogenic. FEBS Lett. 1994; 353:189–193. [PubMed: 7926049]
189. Ponamarev MV, Cramer WA. Perturbation of the Internal Water Chain in Cytochrome *f* of Oxygenic Photosynthesis: Loss of the Concerted Reduction of Cytochromes *f* and b_6. Biochemistry. 1998; 37:17199–17208. [PubMed: 9860833]
190. Robertson DE, Ding H, Chelminski PR, Slaughter C, Hsu J, Moomaw C, Tokito M, Daldal F, Dutton PL. Hydroubiquinone-cytochrome c_2 oxidoreductase from *Rhodobacter capsulatus*: definition of a minimal, functional isolated preparation. Biochemistry. 1993; 32:1310–1317. [PubMed: 8383528]

191. Cape JL, Bowman MK, Kramer DM. A semiquinone intermediate generated at the Q_o site of the cytochrome bc_1 complex: importance for the Q- cycle and superoxide production. Proc Nat Acad Sci USA. 2007; 104:7887–7892. [PubMed: 17470780]
192. Kramer, DM.; Crofts, AR. A Q cycle type model for turnover of the *bf* complex under a wide range of redox conditions. In: Murata, N., editor. Research in Photosynthesis. Kluwer Scientific Publishers; Dordrecht: 1992. p. 491-494.
193. Bowyer JR, Meinhardt SW, Tierney GV, Crofts AR. Resolved difference spectra of redox centers involved in photosynthetic electron flow in *Rhodopseudomonas capsulata* and *Rhodopseudomonas sphaeroides*. Biochim Biophys Acta. 1981; 635:167–186. [PubMed: 6260162]
194. Crofts, AR. The mechanism of the ubiquinol: cytochrome *c* oxidoreductases of mitochondria and of *Rhodopseudomonas sphaeroides*. In: Martonosi, AN., editor. The Enzymes of Biological Membranes. Plenum Press; New York: 1985. p. 347-382.
195. Reece SY, Nocera DG. Proton-coupled electron transfer in biology: results from synergistic studies in natural and model systems. Annu Rev Biochem. 2009; 78:673–699. [PubMed: 19344235]
196. Crofts AR. Proton-coupled electron transfer at the Q_o-site of the bc_1 complex controls the rate of ubihydroquinone oxidation. Biochim Biophys Acta. 2004; 1655:77–92. [PubMed: 15100020]
197. de Vitry C, Desbois A, Redeker V, Zito F, Wollman FA. Biochemical and spectroscopic characterization of the covalent binding of heme to cytochrome b_6. Biochemistry. 2004; 43:3956–3968. [PubMed: 15049703]
198. Bashford CL, Prince RC, Takamiya KI, Dutton PL. Electrogenic events in the ubiquinone-cytochrome bc_2 oxidoreductase of *Rhodopseudomonas sphaeroides*. Biochim Biophys Acta. 1979; 545:223–235. [PubMed: 216398]
199. Bowyer JR, Crofts AR. On the mechanism of photosynthetic electron transfer in *Rhodopseudomonas capsulata* and *Rhodopseudomonas sphaeroides*. Biochim Biophys Acta. 1981; 636:218–233. [PubMed: 6269602]
200. Deisenhofer J, Epp O, Miki K, Huber R, Michel H. X-ray structure analysis of a membrane protein complex. Electron density map at 3 Å resolution and a model of the chromophores of the photosynthetic reaction center from Rhodopseudomonas viridis. J Mol Biol. 1984; 180:385–398. [PubMed: 6392571]
201. Michel H, Epp O, Deisenhofer J. Pigment-protein interactions in the photosynthetic reaction centre from *Rhodopseudomonas viridis*. MBO J. 1986; 5:2445–2451.
202. Deisenhofer J, Michel H. The Nobel lecture: The photosynthetic reaction center from the purple bacterium *Rhodopseudomonas viridis*. The EMBO journal. 1989; 8:2149–2170. [PubMed: 2676514]
203. Jordan P, Fromme P, Witt HT, Klukas O, Saenger W, Krauss N. Three-dimensional structure of cyanobacterial photosystem I at 2.5 A resolution. Nature. 2001; 411:909–917. [PubMed: 11418848]
204. Loll B, Kern J, Saenger W, Zouni A, Biesiadka J. Towards complete cofactor arrangement in the 3.0 Å resolution structure of photosystem II. Nature. 2005; 438:1040–1044. [PubMed: 16355230]
205. Covian R, Trumpower BL. Rapid electron transfer between monomers when the cytochrome bc_1 complex dimer is reduced through center N. J Biol Chem. 2005; 280:22732–22740. [PubMed: 15833742]
206. Gong X, Yu L, Xia D, Yu CA. Evidence for electron equilibrium between the two hemes bL in the dimeric cytochrome bc_1 complex. J Biol Chem. 2005; 280:9251–9927. [PubMed: 15615714]
207. Covian R, Trumpower BL. Regulatory interactions between ubiquinol oxidation and ubiquinone reduction sites in the dimeric cytochrome bc_1 complex. J Biol Chem. 2006; 281:30925–30932. [PubMed: 16908520]
208. Beratan D, Betts JN, Onuchic JN. Protein electron transfer rates set by the bridging secondary and tertiary structure. Science (New York, NY. 1991; 252:1285–1288.
209. Gray HB, Winkler JR. Electron transfer in proteins. Ann Rev Biochem. 1996; 65:537–562. [PubMed: 8811189]

210. Hopfield JJ. Electron Transfer Between Biological Molecules by Thermally Activated Tunneling. Proc Nat Acad Sci USA. 1974; 71:3640–3644. [PubMed: 16592178]

211. Moser CC, Chobot SE, Page CC, Dutton PL. Distance metrics for heme protein electron tunneling. Biochim Biophys Acta. 2008; 1777:1032–1037. [PubMed: 18471429]

212. DeVault, D. Quantum-Mechanical Tunneling in Biological Systems. Cambridge University Press; Cambridge, UK: 1984.

213. Marcus RA, Sutin N. Electron transfers in chemistry and biology. Biochim Biophys Acta. 1984; 811:265–322.

214. Cherepanov DA, Krishtalik LI, Mulkidjanian AY. Photosynthetic electron transfer controlled by protein relaxation: analysis by Langevin stochastic approach. Biophysical journal. 2001; 80:1033–1049. [PubMed: 11222272]

215. Shinkarev VP, Wraight CA. Intermonomer electron transfer in the bc_1 complex dimer is controlled by the energized state and by impaired electron transfer between low and high potential hemes. FEBS Lett. 2007; 581:1535–1541. [PubMed: 17399709]

216. Huang LS, Cobessi D, Tung EY, Berry EA. Binding of the respiratory chain inhibitor antimycin to the mitochondrial bc_1 complex: a new crystal structure reveals an altered intramolecular hydrogen-bonding pattern. J Mol Biol. 2005; 351:573–597. [PubMed: 16024040]

217. Degli Esposti M, Crimi M, Samworth CM, Solaini G, Lenaz G. Resolution of the circular dichroism spectra of the mitochondrial cytochrome bc_1 complex. Biochim Biophys Acta. 1987; 892:245–252. [PubMed: 3036219]

218. Degli Esposti M, Palmer G, Lenaz G. Circular dichroic spectroscopy of membrane haemoproteins. The molecular determinants of the dichroic properties of the *b* cytochromes in various ubiquinol:cytochrome *c* reductases. Eur J Biochem. 1989; 182:27–36. [PubMed: 2543573]

219. Palmer G, Degli Esposti M. Application of exciton coupling theory to the structure of mitochondrial cytochrome *b*. Biochemistry. 1994; 33:176–185. [PubMed: 8286337]

220. Schoepp B, Breton J, Parot P, Vermeglio A. Relative orientation of the Hemes of the Cytochrome bc_1 Complexes from *Rhodobacter sphaeroides*, *Rhodospirillum rubrum* and Beef Heart Mitochondria. J Biol Chem. 2000; 275:5284–5290. [PubMed: 10681500]

221. Hasan, SS.; Zakharov, SD.; Yamashita, E.; Böhme, H.; Cramer, WA. Exciton Interactions between hemes b_n and b_p in the cytochrome b_6f complex. Abstr. 54th Ann. Mtg. Biophysical Soc; February. 2010; San Francisco. 2010.

222. Beratan DN, Onuchic JN, Hopfield JJ. Electron tunneling through covalent and noncovalent pathways in proteins. J Chem Phys. 1987; 86:4488–4498.

223. Beratan, DN.; Onuchic, JN. The protein bridge between redox centers. In: Bendall, DS., editor. Protein Electron Transfer. BIOS Scientific Publishers Ltd; Oxford: 1996. p. 23-42.

224. Gray HB, Winkler JR. Long-range electron transfer. Proc Nat Acad Sci USA. 2005; 102:3534–3539. [PubMed: 15738403]

225. Prytkova TR, Kurnikov IV, Beratan DN. Coupling coherence distinguishes structure sensitivity in protein electron transfer. Science (New York, NY. 2007; 315:622–625.

226. Gray HB, Winkler JR. Electron flow through metalloproteins. Biochim Biophys Acta. 2010; 1797:1563–1572. [PubMed: 20460102]

227. Moser CC, Anderson JL, Dutton PL. Guidelines for tunneling in enzymes. Biochim Biophys Acta. 2010; 1797:1573–1586. [PubMed: 20460101]

228. Lanciano, P.; D-WL; Yang, H.; Darrouzet, E. Inter-monomer electron transfer between the low potential *b* hemes of cytochrome bc_1. personal communication. 2010.

229. Furbacher PN, Girvin ME, Cramer WA. On the question of interheme electron transfer in the chloroplast cytochrome b_6*in situ*. Biochemistry. 1989; 28:8990–8998. [PubMed: 2605237]

230. Hasan, SS.; Zakharov, SD.; Cramer, WA. Preferred Pathway of Electron Transfer in the Dimeric Cytochrome b6f Complex: Selective Reduction of One Monomer; Abstract. 55th Ann. Mtg. Biophysical Soc; March, 2011; Baltimore. 2011.

231. Deisenhofer J, Epp O, Sinning I, Michel H. Crystallographic refinement at 2.3 Å resolution and refined model of the photosynthetic reaction centre from *Rhodopseudomonas viridis*. Journal of Molecular Biology. 1995; 246:429–457. [PubMed: 7877166]

232. Wohri AB, Wahlgren WY, Malmerberg E, Johansson LC, Neutze R, Katona G. Lipidic sponge phase crystal structure of a photosynthetic reaction center reveals lipids on the protein surface. Biochemistry. 2009; 48:9831–9838. [PubMed: 19743880]

233. Guskov A, Kern J, Gabdulkhakov A, Broser M, Zouni A, Saenger W. Cyanobacterial photosystem II at 2.9-A resolution and the role of quinones, lipids, channels and chloride. Nat Struct Mol Biol. 2009; 16:334–342. [PubMed: 19219048]

234. Aird A, Wrachtrup J, Schulten K, Tietz C. Possible pathway for ubiquinone shuttling in *Rhodospirillum rubrum* revealed by molecular dynamics simulation. Biophys J. 2007; 92:23–33. [PubMed: 17028136]

235. Li Y, Zhou Z, Post CB. Dissociation of an antiviral compound from the internal pocket of human rhinovirus 14 capsid. Proc Nat Acad Sci USA. 2005; 102:7529–7534. [PubMed: 15899980]

236. Draber W, Trebst A, Harth E. On a new inhibitor of photosynthetic electron-transport in isolated chloroplasts. Z Naturforsch B. 1970; 25:1157–1159. [PubMed: 4394873]

237. Malkin R. Interaction of photosynthetic electron transport inhibitors and the Rieske Iron-Sulfur center in chloroplasts and the cytochrome b6-f complex. Biochemistry. 1982; 21:2945–2950. [PubMed: 7104304]

238. Roberts AG, Kramer DM. Inhibitor double occupancy in the Q_o pocket of the chloroplast cytochrome b_6f complex. Biochemistry. 2001; 40:13407–13412. [PubMed: 11695886]

239. Roberts AG, Bowman MK, Kramer DM. The inhibitor DBMIB provides insight into the functional architecture of the Q_o site in the cytochrome b_6f complex. Biochemistry. 2004; 43:7707–7716. [PubMed: 15196013]

240. Yan J, Kurisu G, Cramer WA. Intraprotein transfer of the quinone analogue inhibitor 2,5-dibromo-3-methyl-6-isopropyl-p-benzoquinone in the cytochrome b6f complex. Proceedings of the National Academy of Sciences of the United States of America. 2006; 103:69–74. [PubMed: 16371475]

241. Whitelegge JP, Zhang H, Taylor R, Cramer WA. Full subunit coverage liquid chromatography electrospray-ionization mass spectrometry ($LCMS^+$) of an oligomeric membrane protein complex: the cytochrome b_6f complex from spinach and the cyanobacterium. M laminosus, Mol Cell Prot. 2002; 1:816–827.

242. von Heijne G. Membrane proteins: from sequence to structure. Ann Rev Biophys Biomolec Struct. 1994; 23:167–192.

243. Gasteiger E, Gattiker A, Hoogland C, Ivanyi I, Appel RD, Bairoch A. ExPASy: The proteomics server for in-depth protein knowledge and analysis. Nucleic Acids Research. 2003; 31:3784–3788. [PubMed: 12824418]

244. Dutton PL, Jackson JB. Thermodynamic and kinetic characterization of electron transfer components *in situ* in *Rhodopseudomonas spheroides* and *Rhodospirillum rubrum*. Euro J Biochem. 1972; 30:495–510.

245. Petty KM, Dutton PL. Ubiquinone-cytochrome *b* electron and proton transfer: a functional pK on cytochrome b_{50} in *Rhodopseudomonas sphaeroides* membranes. Arch Biochem Biophys. 1976; 172:346–353. [PubMed: 4015]

246. T'Sai AL, Palmer G. Potentiometric studies on yeast complex III. Biochim Biophys Acta. 1983; 722:349–363. [PubMed: 6301554]

247. Rich PR, Jeal AE, Madgwick SA, Moody AJ. Inhibitor effects on redox-linked protonations of the *b* haems of the mitochondrial bc_1 complex. Biochim Biophys Acta. 1990; 1018:29–40. [PubMed: 2165418]

248. Yun CH, Crofts AR, Gennis RB. Assignment of the histidine axial ligands to the cytochrome bH and cytochrome bL components of the bc_1 complex from *Rhodobacter sphaeroides* by site-directed mutagenesis. Biochemistry. 1991; 30:6747–6754. [PubMed: 1648391]

249. Yun CH, Van Doren SR, Crofts AR, Gennis RB. The use of gene fusions to examine the membrane topology of the L-subunit of the photosynthetic reaction center of the cytochrome *b* subunit of the bc_1 complex from *Rhodobacter sphaeroides*. J Biol Chem. 1991; 266:10967–10973. [PubMed: 1645718]

250. Gray KA, Dutton PL, Daldal F. Requirement of histidine 217 for ubiquinone reductase activity (Qi site) in the cytochrome bc_1 complex. Biochemistry. 1994; 33:723–733. [PubMed: 8292600]

251. Hurt E, Hauska G. Identification of the polypeptides in the cytochrome b_6f complex from spinach chloroplasts with redox-center-carrying subunits. J Bioenerg Biomemb. 1982; 14:405–424.
252. Hurt EC, Hauska G. Cytochrome-B6 from Isolated Cytochrome-B6f Complexes - Evidence for 2 Spectral Forms with Different Midpoint Potentials. Febs Letters. 1983; 153:413–419.
253. Rich PR, Madgwick SA, Moss DA. The interactions of duroquinol, DBMIB, and NQNO with the chloroplast cytochrome *bf* complex. Biochim Biophys Acta. 1991; 1058:312–328.
254. Pierre Y, Breyton C, Kramer D, Popot JL. Purification and characterization of the cytochrome b_6f complex from *Chlamydomonas reinhardtii*. J Biol Chem. 1995; 270:29342–29349. [PubMed: 7493968]
255. Bohme H, Cramer WA. Uncoupler-dependent decrease in midpoint potential of the chloroplast cytochrome b_6. Biochim Biophys Acta. 1973; 325:275–283. [PubMed: 4761984]
256. Bohme H. Photoreactions of cytochrome b_6 and cytochrome *f* in chloroplast photosystem I fragments. Z Naturforsch. 1976; 31:68–77.
257. Rich PR, Bendall DS. The redox potentials for the *b*-type cytochromes of higher plant chloroplasts. Biochim Biophys Acta. 1980; 591:153–161. [PubMed: 7388012]
258. Kramer DM, Crofts AR. Re-examination of the properties and function of the *b* cytochromes of the thylakoid cytochrome *bf* complex. Biochim Biophys Acta. 1994; 1184:193–201.
259. Nelson ME, Finazzi G, Wang QJ, Middleton-Zarka KA, Whitmarsh J, Kallas T. Cytochrome b_6 arginine 214 of *Synechococcus sp*. PCC 7002, a key residue for quinone-reductase site function and turnover of the cytochrome *bf* complex. J Biol Chem. 2005; 280:10395–10402. [PubMed: 15632120]
260. Joliot P, Joliot A. Electron transfer between the two photosystems. Biochimi Biophys Acta. 1984; 765:210–218.
261. Joliot P, Joliot A. Slow electrogenic phase and intersystem electron transfer in algae. Biochimi Biophys Acta. 1985; 806:398–409.
262. Joliot P, Joliot A. Electron transfer between photosystem II and the cytochrome *b/f* : mechanistic and structural implications. Biochimi Biophys Acta. 1992; 1102:53–61.
263. Kassner RJ. Effects of nonpolar environments on the redox potentials of heme complexes. Proc Nat Acad Sci USA. 1972; 69:2263–2267. [PubMed: 4506096]
264. Cramer WA, Whitmarsh J. Photosynthetic cytochromes. Ann Rev Plant Physiol. 1977; 28:133–172.
265. Krishtalik LI, Tae GS, Cherepanov DA, Cramer WA. The redox properties of cytochromes *b* imposed by the membrane electrostatic environment. Biophysical journal. 1993; 65:184–195. [PubMed: 8396453]

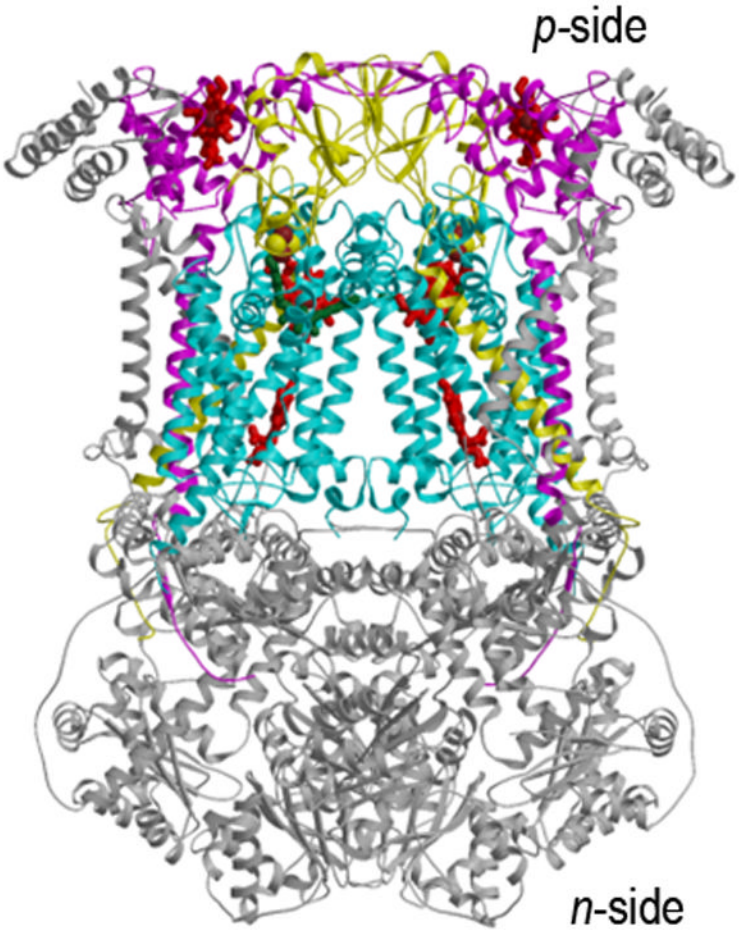

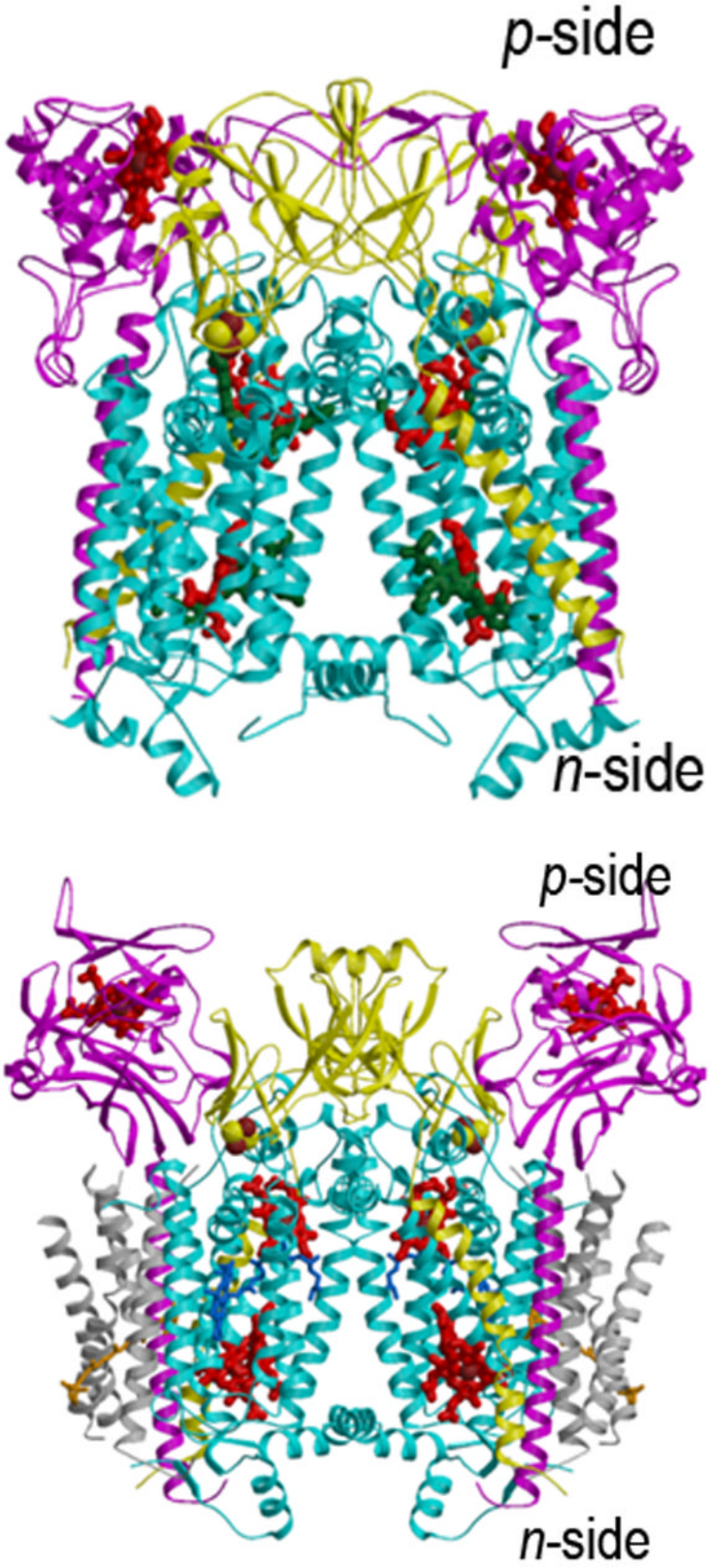

Fig. 1.

Structures of the cytochrome bc_1 complex from the electron transport chain of **(A)** yeast mitochondria (PDB: 3CX5(15)), and **(B)** the purple photosynthetic bacterium, *Rb. sphaeroides*, with bound antimycin and stigmatellin (2QJP, (14)); (**C**) native b_6f complex from the cyano-bacterium, *M. laminosus* (2E74, (19)). The ribbon diagrams show the common central structure. Color code: (yellow) Rieske protein with cluster-containing peripheral domain on one monomer and its TMH spanning the width of the other; other colors: b_6f -cyt *f* and bc_1-cyt. c_1, magenta; cyt *b* and b_6f -subunit IV, cyan.

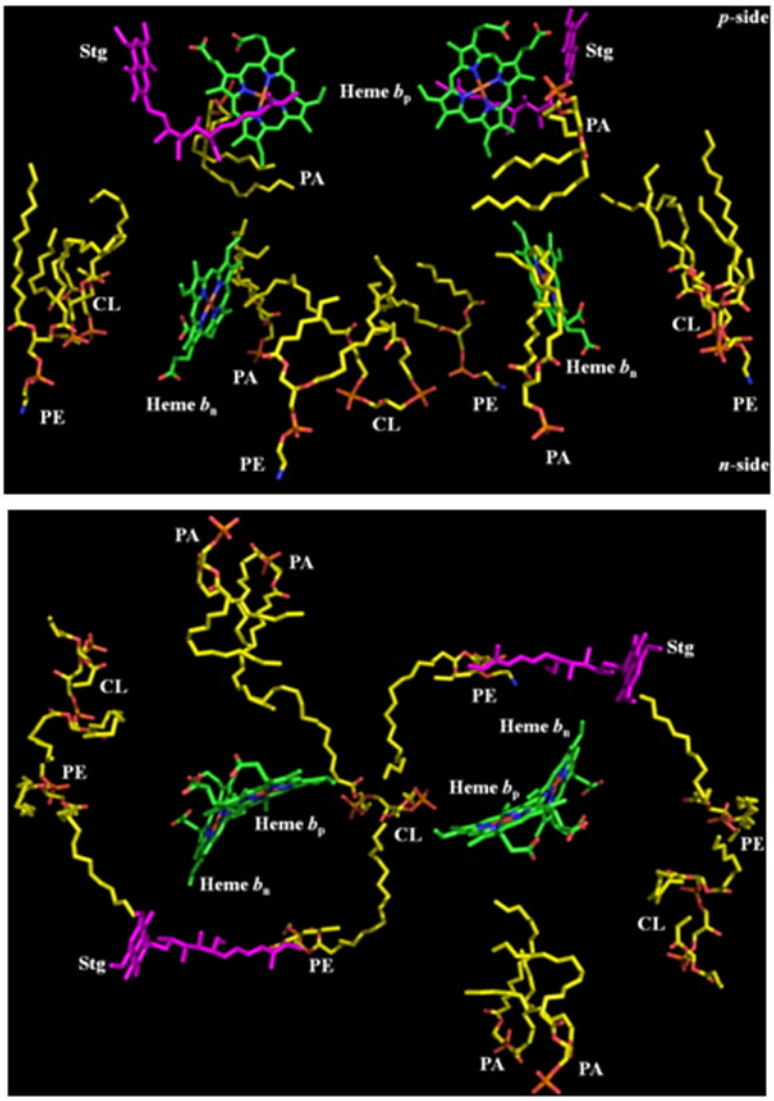

Fig. 2.

Arrangement of lipids, 2 PE, 2 PA, 1.5 CL per monomer, in the yeast cytochrome bc_1 complex (PDB, 3CX5; (15)); (A) side and (B) top view. 1.5 molar stoichiometry of cardiolipin (CL), determined from the 3CX5 crystal structure, is a consequence of sharing one CL at the n-side interface between the two monomers.

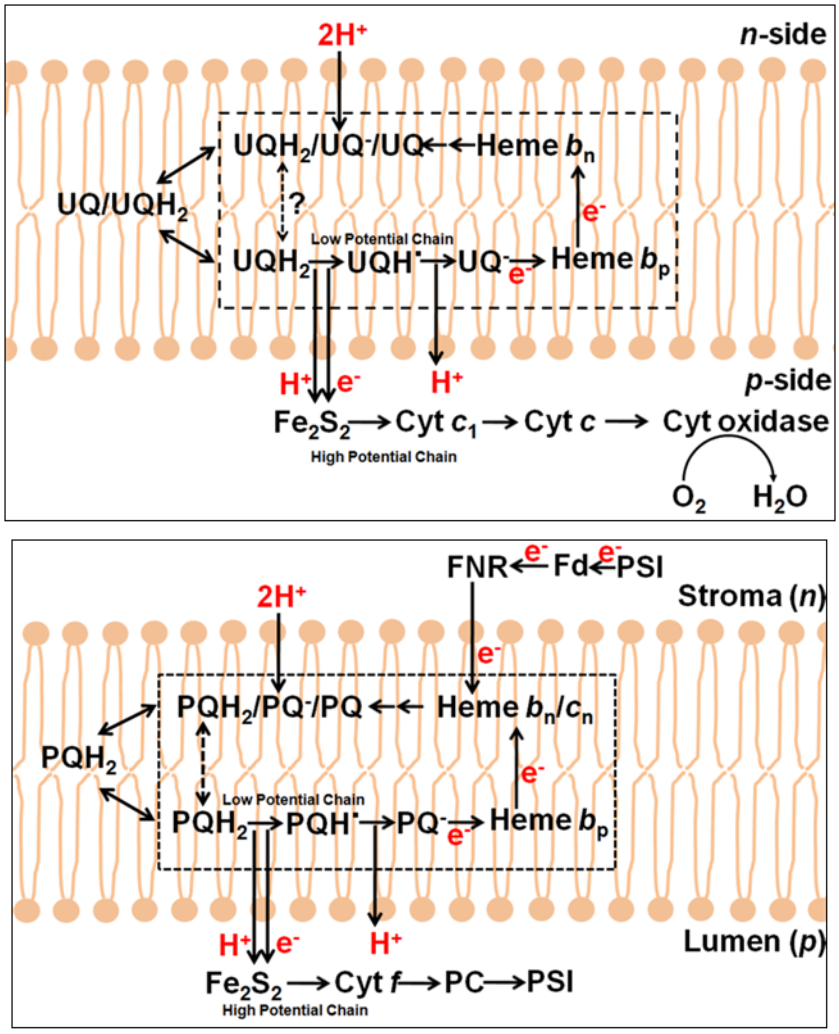

Fig. 3.

Q cycle models for electron transfer and proton translocation through (**A**) the bc_1 complex in the respiratory chain (176) and the purple photosynthetic bacteria,(48) (reaction sequence (Table 3A1-3) and (**B**) the b_6f complex that functions in oxygenic photosynthesis (Table 3B). The original "Q cycle" model (172, 174) for proton translocation, formulated in the aftermath of the experiment of the discovery of oxidant-induced reduction of heme *b* (171), focused on the mitochondrial bc_1 complex. Fundamental features of the classical Q cycle are: (**i**) the [2Fe-2S] complex on the *p*-side of the complex that functions as the one electron oxidant of the two electron lipophilic quinol electron and proton donor, resulting in a bifurcated pathway into high and low potential chains; (**ii**) the high potential segment of the bifurcated pathway, initiated by electron transfer to cytochrome c_1 or *f*, which transfers one electron to the high potential electron terminal acceptor, (**A**) cytochrome oxidase or (**B**) photosystem I, while generating the semiquinone; (**iii**) the semiquinone donates the second electron to the two trans-membrane hemes *b*, b_p and b_n, in the low potential segment of the bifurcated chain that reduces a quinone or semiquinone (53) bound at the Q_n site.

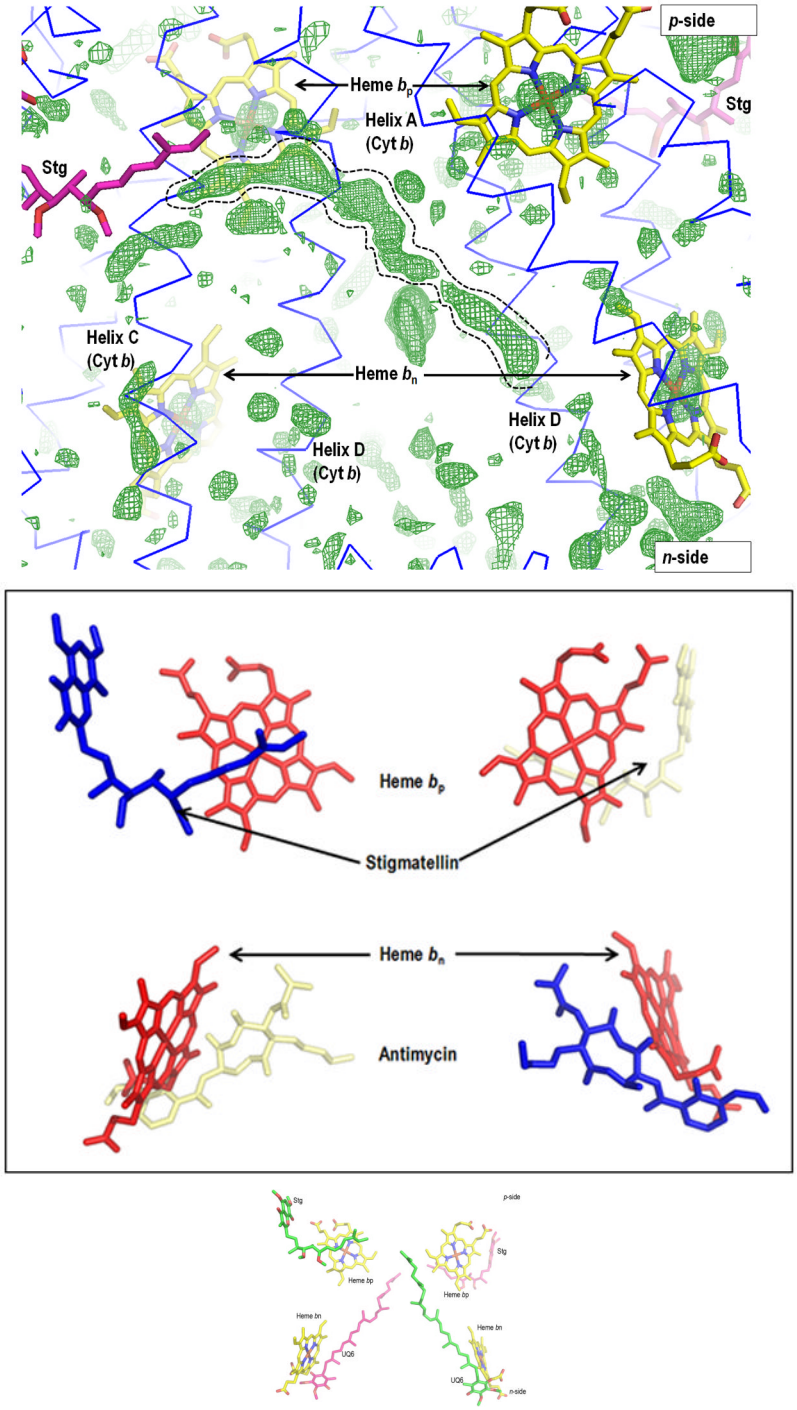

Fig. 4.

(**A**) Presence of lipid-like molecules in the inter-monomer cavity of yeast cytochrome bc1 complex (PDB 3CX5). The outlined density may correspond to an acyl chain of a lipid or detergent molecule or it may be attributed to the isoprenoid tail of a ubiquinone molecule (as found in the ^{Q}n site of the yeast ^{bc}1 complex (PDB, 1KB9). Figure generated in PyMol from PDB 3CX5 and its Fo-Fc map contoured at + 3.0 sigma. Negative densities were not included in the analysis. (**B**) n- and p- side binding sites of quinone analogue inhibitors,

antimycin A and stigmatellin [PDB: 1PPJ (216) or 1NTZ (10), which are on the same side (yellow or blue) of the dimeric complex, implying that if a *trans*-complex quinone pathway operates for electron and proton transfer, it would be inter-monomer. (**C**) Yeast bc_1 complex (PDB 1KB9) showing (side-view) cross-over of ubiquinone isoprenoid tail (UQ-6, bound at Q_n site) from one monomer across the inter-monomer cavity, to the Qp site portal in the other monomer, located by presence of quinone analog stigmatellin (Stg). The Stg and UQ-6 pair colored magenta is positioned on one face of the bc_1 dimer, while that colored green lies on the other.

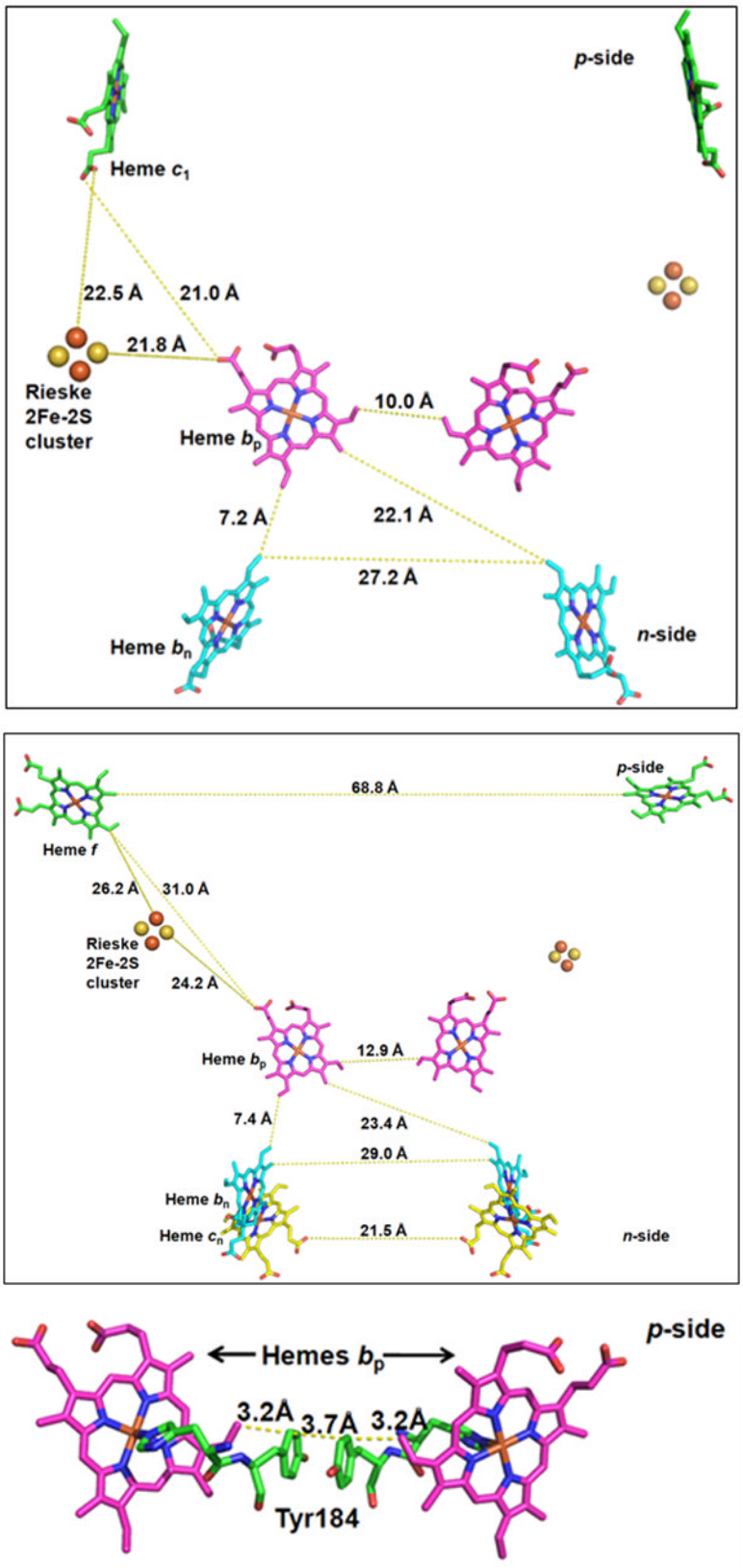

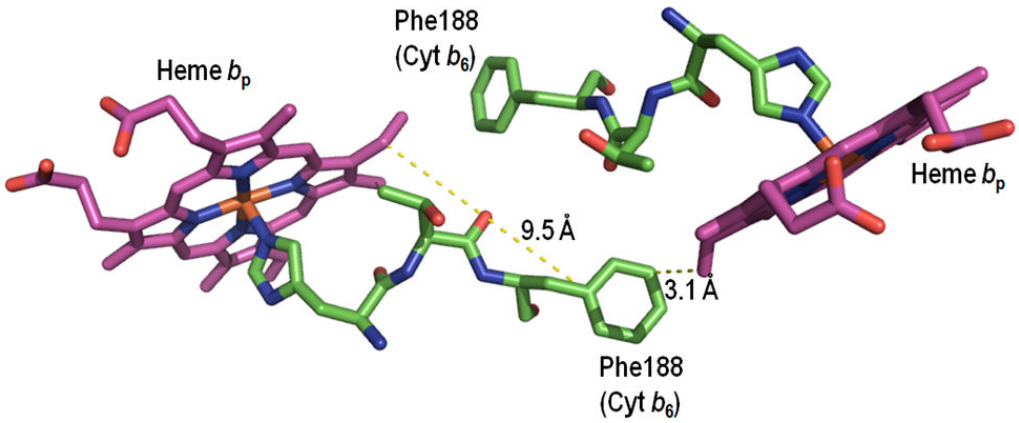

Fig. 5.

Possible pathways for electron transfer. Intra-and inter-monomer edge-edge distances for: **(A)** yeast bc_1 (PDB: 3CX5); (**B**) cyanobacterial b_6f (PDB: 2E74) complex. (**C, D**) Center-center (Fe-Fe) connection via histidine ligands, and (**C**) an intra-monomerTyr184–Tyr184 bridge in yeast bc_1 (PDB 3CX5), and (**D**) a Phe188–Phe188 bridge in the *M. laminosus* b_6f complex.

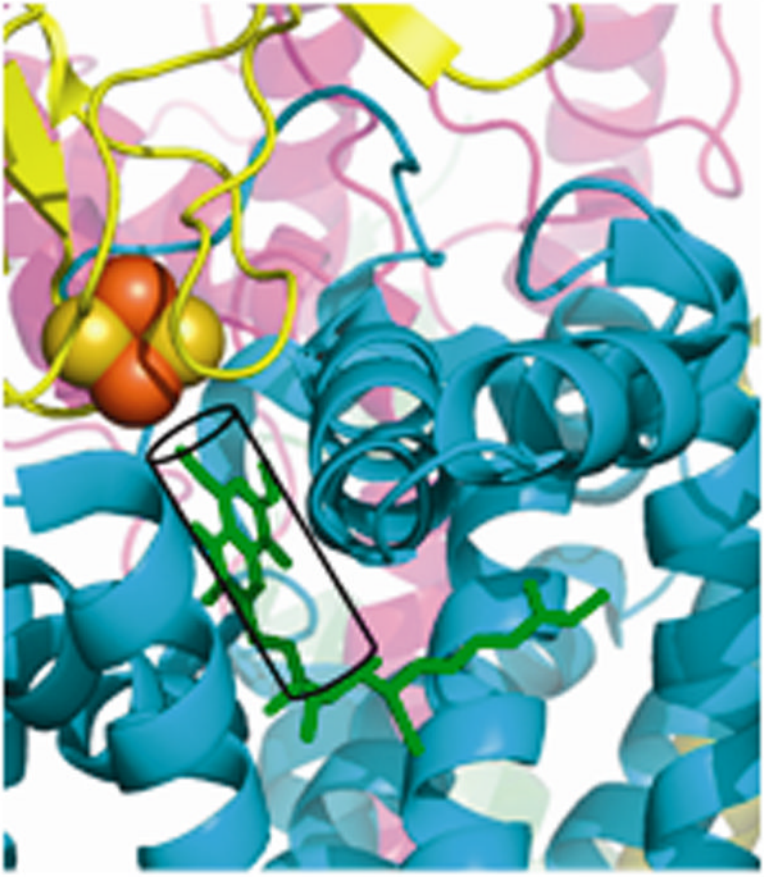

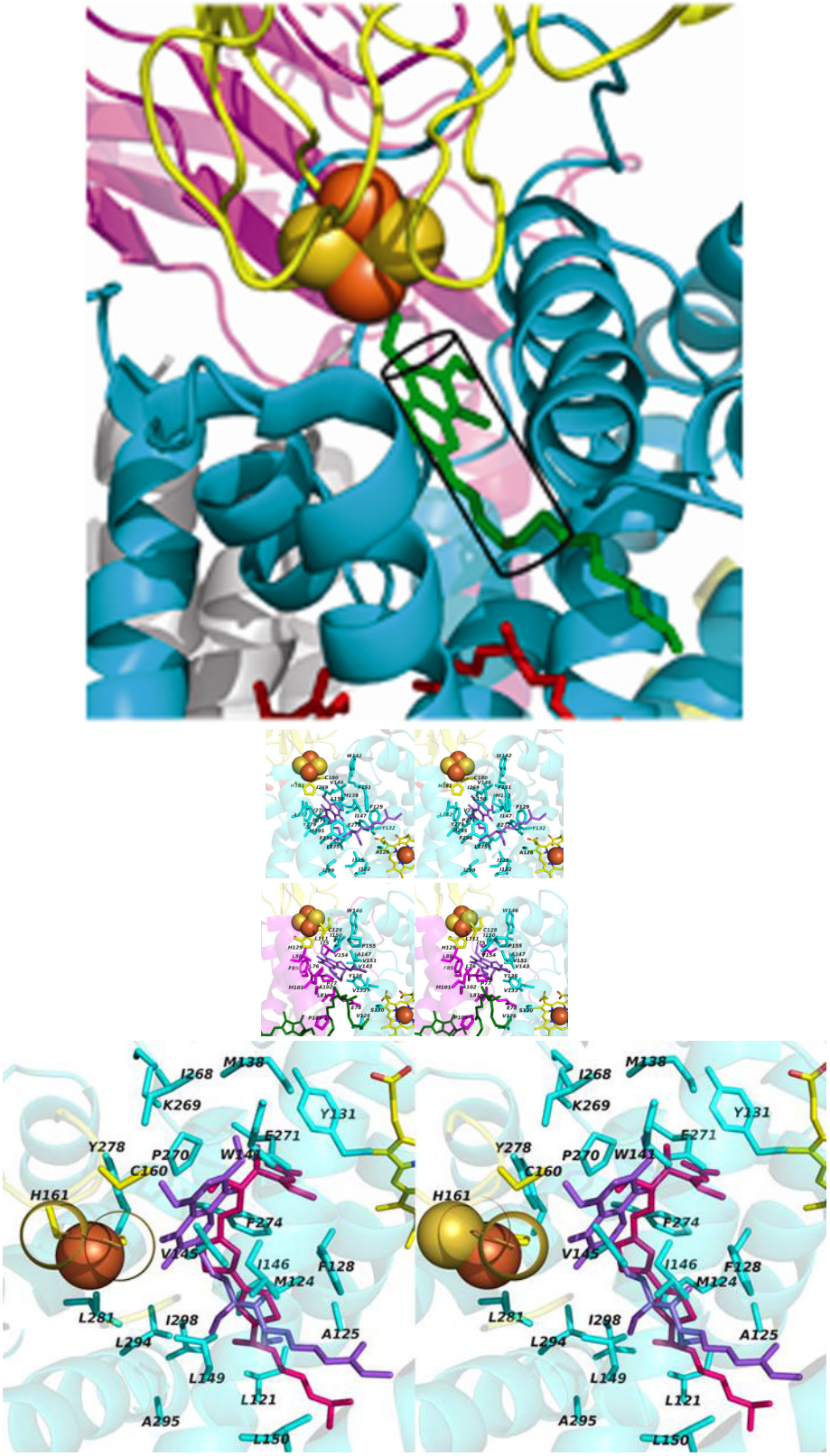

Fig. 6.

Narrow p-side quinol/quinone binding niche to access/exit the p-side [2Fe-2S] electron/proton acceptor in cytochrome *bc* complexes: (**A**): Stigmatellin (green) in a p-side portal in cytochrome bc_1 complex (PDB 3CX5); (**B**) Tridecyl-stigmatellin (green) in a narrow portal near the p-side of the *M. laminosus* cyt b_6f complex (PDB, 2E76); chlorophyll *a* shown in red, partly occluding the portal; (**C**, **D**) Expanded views (stereo) of p-side Q/QH_2 entry/exit portal showing all residues within 4 Å of stigmatellin (colored violet, as in panels A, B) in (**C**) the yeast bc_1 (PDB 3CX5) complex, and (**D**) the *M. laminosus* b_6f complex (PDB: 2E76), showing the residues around tridecyl-stigmatellin (colored violet); the chlorophyll *a* phytyl chain (colored green) is shown occupying a portion of the portal. (**E**) Overlap (stereo) of p-side stigmatellin (PDB: 1SQX) and myxathiozol (1SQP) sites in the bovine mitochondrial bc_1 complex.

Table I

Subunit composition and pI values of the eight polypeptide subunits of the *M. laminosus* cyanobacterial cytochrome b_6f complex (PDB: 2E74); consensus mid-point oxidation-reduction potentials of prosthetic groups

Subunit[a]	*M. laminosus* subunit mol wt, kDa (241)	*C. reinhardtii* subunit mol wt, kDa	pI[b] (*M. laminosus*)	pI(*C. reinhardtii*)[c]	E_{m7} (mV)[c]
Cyt f (1 heme)	32.273	31.249	6.7	8.3	+ 350 − 380
Cyt b_6 (3 hemes)	24.712	24.165	9.0	8.8	(−50 (b_n); −50 - −150 (b_p); + 100 (heme c_n)[d]
ISP [2Fe-2S]	19.295	18.333	6.8	5.8	+ 300 (pH 6.5) - + 320
suIV	17.528	17.295	8.1	6.6	--
PetG	4.058	3.984	4.5	4.4	--
PetM	3.841	4.036	10.4	4.3	--
PetL	3.530	3.436	10.2	9.5	--
PetN	3.304	3.282	5.7	6.0	--

[a] Subunits listed are the tightly bound subunits seen in the crystal structures of the complex;

[b] pI values include extrinsic and hydrophobic integral domains; the basic pK's of suIV and cyt b_6 arise partly from an excess of basic residues on the n-or stromal side of the membrane, the side from which these subunits are predicted to be inserted into the membrane (242); pI values determined for the complex in *M. laminosus* (PDB, 1Q90) using ExPASy (243).

[c] Redox potentials of 2 *b* hemes: in contrast to bc_1 complexes (244–249, 190, 250, 58), for which the ΔE_m between hemes b_n and b_p is sufficiently resolved ($\Delta E_m \approx 125$–150 mV) to define b_h (*b*-high potential) and b_l (*b*-low potential) hemes, redox titration data do not clearly allow this inference for the b_6f complex. There is a discrepancy between titrations of the b_6f complex *in vitro*, for which a measurable $\Delta E_m \approx 100$ mV is consistently resolved (251–254, 130), and a number of *in situ* (in membrane) titrations that do not show resolved b_n and b_l ($\Delta E_m \leq 50$ mV) (255–257, 187, 229, 253). Two studies on *in situ* titrations report two resolved *b* heme components (258, 259), and a large ΔE_m has been inferred in studies on the slow electrochromic phase (260–262, 192, 186, 79), and biphasic kinetics of heme reduction (105). Regarding the more negative E_m values obtained for one of the *b* hemes titrated i*n vitro*, it could result from solvent exposure (263), as shown for cytochrome *b*-559 in the PS II reaction center (264, 265).

[d] for heme c_n, titration *in vitro* inidicates the ΔE_m between hemes c_n/b_n is ~ 150 mV (130); *in vivo*, ΔE_m 20 mV (105). [e] E_{m7} for Q redox reactions: (i) $UQ + 2e^- + 2\,H^+ \rightarrow UQH_2$, + 65 mV; (ii) $PQ + 2e^- + 2\,H^+ \rightarrow PQH_2$, + 100 mV; (iii) $UQ + e^-$, $\rightarrow UQ^{\bullet -}$, ~ −150 mV; (iv) $PQ + e^- \rightarrow PQ^{\bullet -}$, ~ −100 mV.

Table 2

Number of amino acids in close contact (< 4 Å) between the two monomers in the dimeric $^{bc}1$ and $^{b}6^{f}$ complexes

Structure	**3CX5**	**1NTZ**	**2QJP**	**2E74**	**2ZT9**
Close contact, aa pairs	131	120	80	65	66
Cytochrome *b*	48	44	55	39	43
b_6f -subunit IV	--	--	--	10	8
Rieske [2Fe-2S]	23	16	25	16	15
bc_1-subunit I	6	1	--	--	--
bc_1-subunit II	26	24	--	--	--
bc_1-Cytochrome c1	9	11	--	--	--
bc_1-14KDa protein	10	14	--	--	--
yeast- bc_1-subunit VIII	9	--	--	--	--
bovine- bc_1- Subunit XI	--	10	--	--	--

Table 3

(A1-A3) Oxidant-induced reduction, electron transfer through the high potential chain, and trans-membrane electron transfer in bc complexes. (B1-B4) n-side reduction of UQn, PQn.1

A1. *p*-side quinol oxidation* (Q is PQH_2 in b_6f and UQH_2 in bc_1 complexes)

$UQ_pH_2 + FeS(o) \rightarrow UQ_p^{\bullet -} + FeS(r) + 2H^+$

$UQ_p^{\bullet -} + b_p(o) \rightarrow UQ_p + b_p(r)$

A2. high potential chain (to the soluble acceptor, cytochrome *c* or plastocyanin**)**

$FeS(r)$ + cyt $c_1(o) \rightarrow FeS(o)$ + cyt $c_1(r)$; involves rotation-translation of ISP (5);

cyt $c_1(r)$ + cyt $c(o) \rightarrow$ cyt $c_1(o)$ + cyt $c(r)$

A3. trans-membrane *p*- to *n*-side electron transfer

heme $b_p(r)$ + heme $b_n(o) \rightarrow b_p(o) + b_n(r)$

B1. n-side reduction of UQ_n or PQ_n by consecutive transfer of 2 electrons (2 one-electron transfers) from the *p*-side;

- **i.** heme $b_n(r) + UQ_n \rightarrow UQ_n^{\bullet -}$; transfer of 1 electron arising from oxidation of UQ_pH_2
- **ii.** heme $b_n(r) + UQ_n^{\bullet -} + 2H^+ \rightarrow$ heme $b_n(o) + UQ_nH_2$; transfer of 2^{nd} electron from 2^{nd} UQ_pH_2.

B2. *n*-side 2 electron reduction of PQ_n by consecutive transfer of 2 electrons from the *p*-side, resulting from oxidation of two PQ_pH_2 and cooperative 2 electron reduction of PQ_n transfer via hemes b_p and b_n

$b_p(r) + b_n(r) + UQ_n + 2H^+ \rightarrow$ heme $b_n(o)$ + heme $b_n(o) + UQ_nH_2$; (2 electron reduction of ubiquinone avoids the 1 electron reduction of UQ that may be energetically uphill; (194)).

B3. *n*-side 2 electron reduction of PQ by 2 electrons from *p*-side via heme b_n (r)/c_n(r), or 1 electron from p-side and 1 from *n-side* (via ferredoxin/FNR)(75, 76, 80**)**

- **i.** heme $b_p(r)$ + heme $b_n(o) \rightarrow b_p(o) + b_n(r)$
- **ii.** $b_n(r)$ /$c_n(o) \rightarrow b_n(o)/c_n(r)$; the more positive potential of heme c_n relative to heme b_n (130) could facilitate this transfer; then, in a second p- to n-side transfer,
- **iii.** $b_p(r)$ + heme $b_n(o)/c_n(r) \rightarrow b_n(r)/c_n(r)$
- **iv.** $b_n(r)/c_n(r) + PQ_n + 2\ H^+ \rightarrow b_n(o)/\ c_n(o) + PQ_nH_2$, or, via the PSI-linked cyclic pathway,
- **v.** $Fd/FNR(r) + b_n(o)/c_n(r)/PQ_n \rightarrow Fd/FNR(o) + b_n(r)/c_n\ (r)/PQ_n$
- **vi.** $b_n(r)/c_n(r)/PQ_n + 2\ H^+ \rightarrow b_n(o)/c_n(o)/PQ_nH_2$ *o, oxidized; r, reduced];

B.4. "Activated Q cycle"; *bc* complex "primed" by n-side 2 electron reduction by membrane pool quinol of Q_n to Q_nH_2 in one monomer (1) and, via inter-monomer transfer, of heme b_n to b_n (r) (2) in the other (53, 80).

- **i.** QH_2 (pool) + $Q_n \rightarrow$ Q (pool) + Q_nH_2 [monomer 1]
- **ii.** Q_nH_2 [monomer 1] + $b_n(o)$ [monomer 2] $\rightarrow Q_n^{\bullet -}$ [monomer 1] + $b_n(r)$ [monomer 2] + $2H^+$
- **iii.** $Q_n^{\bullet -}$ [1] reduction to Q_nH_2 by a single p-side turnover using reactions A1-3 and B1 above.

Table 4

Inter- and intra-monomer distances between the two hemes b_p and b_p/b_n of the dimeric cytochrome *bc* complexes: the bc_1 complex (PDB: 3CX5, 2A06, yeast and bovine mitochondria with the p-side quinone-analogue inhibitor stigmatellin; 1NTZ, bovine complex with ubiquinone-2 bound at the Q_n site; 2QJP, purple photosynthetic bacterium, *Rb. sphaeroides*, with bound p-side stigmatellin and n-side antimycin); b_6f complexes: (2ZT9, 2E74), native structures from two different cyanobacteria, *M. laminosus* and Anabaena 7120, and from the green alga, *C. reinhardtii* with tridecyl-stigmatellin (1Q90)

PDB code	**3CX5**	**2A06**	**1NTZ**	**2QJP**	**2E74**	**2ZT9**	**1Q90**
Resolution (Å)	1.9	2.1	2.60	2.60	3.0	3.0	3.1
R factors	0.245	0.222	0.247	0.244	0.222	0.230	0.222
	0.263	0.258	0.283	0.277	0.268	0.259	0.261
Coordinate error (Å)	0.31	0.29	0.47	0.41	0.44	0.44	0.43
A. Inter-monomer distances (Å)							
heme b_p - heme b_p (edge-edge)	10.0	10.5	10.9	10.6	12.9	12.7	12.7
heme b_p - heme b_p (ring - ring)	13.7	14.3	13.8	13.4	15.2	15.1	15.1
heme b_p–heme b_p(center-center)	21.2	21.4	20.7	20.7	22.0	22.1	22.0
B. Intra-monomer distances (Å)							
heme b_p - heme b_n (edge –edge)	7.2	7.0	8.6	7.9	7.4	8.2	8.9
heme b_p – heme b_n (ring-ring)	12.2	12.0	12.3	11.9	12.2	12.0	12.2
heme b_p – heme b_n (center-center)	20.7	20.4	20.6	20.4	20.6	20.7	20.8